The Effect of Interactive Clouds and Radiation on Convection Activity in a Numerical Model of the Tropics

by

Julia M. Slingo

U.K. METEOROLOGICAL OFFICE, BRACKNELL, ENGLAND

1. Introduction

The aim of any parameterization of cumulus convection is to represent the collective influence of an ensemble of cumulus clouds on the large-scale environment. It is generally accepted that cumulus convection modifies the large-scale temperature and moisture fields through detrainment and cumulus induced subsidence in the environment (Gray, 1972; Yanai et al, 1973; Arakawa and Schubert, 1974). The detrainment causes large-scale cooling and moistening and cumulus induced subsidence, large-scale warming and drying. The net effect of this on the environment can be assessed by considering the budgets of dry static energy ($s = C_p T + gs$) and water vapour (q) for a horizontal area large enough to contain an ensemble of cumulus clouds:

$$\frac{\partial \bar{s}}{\partial t} + \overline{\nabla . s\underline{v}} + \frac{\partial \overline{s\omega}}{\partial p} = Q_R + L(c-e) \qquad (1)$$

$$\frac{\partial \bar{q}}{\partial t} + \overline{\nabla . q\underline{v}} + \frac{\partial \overline{q\omega}}{\partial p} = e - c \qquad (2)$$

where Q_R = radiative heating rate

c = condensation rate

e = evaporation rate

From (1) and (2) an apparent heat source Q_1 and an apparent moisture sink Q_2 can be derived such that

$$Q_1 = Q_R + L(c-e) - \frac{\partial \overline{s'\omega'}}{\partial p} \qquad (3)$$

$$Q_2 = L(c-e) + L\frac{\partial}{\partial p}\overline{q'\omega'} \qquad (4)$$

Combining these to obtain the net heating Q by cumulus convection:

$$Q = Q_1 - Q_R - Q_2 = -\frac{\partial}{\partial p}\overline{(s' + Lq')\omega'} = -\frac{\partial}{\partial p}\overline{h'\omega'} \qquad (5)$$

where h is the moist static energy ($\equiv Lq + C_p T + gz$). $\overline{h'\omega'}$ is the vertical eddy transport of heat and may be used to measure the activity of cumulus convection. Estimates of Q_1, Q_2 and Q_R by Yanai et al (1973) (Fig. 1) show that the magnitudes of $|Q_1 - Q_2|$ and $|Q_R|$ are comparable, indicating the need for accurate estimates

of radiative heating rates. In addition Yanai et al (1976) have shown that radiative cooling alone is sufficient to force a substantial part of the cloud base mass flux for shallow clouds and the secondary maximum associated with deep clouds (Fig. 2). This result was obtained using a radiative heating rate profile given by Dopplick (1970) for clear skies. They also showed that the cloud base mass flux was sensitive to the radiative heating profile (Fig. 3) although its bimodal distribution appeared to be a feature of the maritime tropical atmosphere.

The validity of using a clear sky radiative heating profile has not been considered in the literature. The effects of clouds on the radiative heating profile can be substantial as is shown by Fig. 4, taken from Fimpel et al (1977), where observed infrared heating rates under different sky conditions are given. In the vicinity of a cloud cluster, for example, it is likely that clouds, other than convective clouds, will be present. A perturbed heating rate profile would therefore be more appropriate than that for a clear sky. The purpose of this paper is to try and assess the effect of cloud modulated radiative heating rates on convective acitivity in a numerical model of the tropics which includes a fully interactive cloud and radiation scheme.

2. The model

The model used was a version of the 11-layer limited area tropical model developed for use in GATE and described by Lyne and Rowntree (1976) and Lyne et al (1976). The vertical coordinate is $\sigma \equiv P/P_*$ where P is the pressure and P_*, the pressure at the earth's surface. The boundaries and nominal central levels of layers are specified in Table 1.

Table 1 - Layer boundaries and nominal levels in σ-coordinates

	11	10	9	8	7	6	5	4	3	2	1	
Layer Boundaries	1.0	.975	.90	.79	.65	.51	.37	.27	.195	.125	.06	0
Nominal level	.987	.937	.844	.718	.578	.436	.317	.230	.157	.089	.022	

In the horizontal, variables are represented on a 2° latitude-longitude mesh with boundary rows along 35N, 15S, 77W and 49E. The model includes the interactive radiation scheme, described in detail by Walker (1977), which allows for low, medium, high and convective clouds. A typical cloud configuration is shown in Fig. 5. The

random. The radiative properties for each cloud type are shown in Table 2. The emissivity of cirrus cloud has been increased from 0.5 to 1.0 for the experiments reported here since tropical cirrus, arising from cumulonimbus outflow is generally thicker and more opaque than extra-tropical cirrus. The assumption of black cirrus is supported by the results of Griffith and Cox (1977) based on aircraft measurements of cirrus cloud microphysics with simultaneous radiometric observations made during GATE.

Table 2 - Radiative properties of clouds

Cloud Type	Reflectivity	Transmissivity	Absorptivity	Emissivity
High	0.2	0.75	0.05	1.0
Medium	0.6	0.3	0.1	1.0
Low	0.7	0.2	0.1	1.0
Convective	0.7	0.2	0.1	1.0

The cloud parameterisation has been based on studies of GATE data and the amount and height of each cloud predicted using model variables and parameters from the penetrative convection scheme (Walker 1978). The following functions of relative humidity (R) and lapse rate ($\partial\theta/\partial p$) are used for predicting cloud amount:

High Cloud $$C_H = \frac{1}{400}(R-80)^2 \quad \text{for } R \geq 80\% \qquad (6)$$

Medium Cloud $$C_M = \frac{1}{1225}(R-65)^2 \quad \text{for } R \geq 65\% \qquad (7)$$

Low Cloud (a) $$C_L = \frac{1}{400}(R-80)^2 \quad \text{for } R \geq 80\% \text{ and } \partial\theta/\partial p \geq -0.07 \qquad (8a)$$

(b) $$C_L = -16.67\frac{\partial\theta}{\partial p} - 0.1167 + \frac{\delta}{400}(R-80)^2 \qquad (8b)$$

for $\partial\theta/\partial p < -0.07$ and where $\delta = 1$ for $R \geq 80\%$

otherwise $\delta = 0$

Convective Cloud $$C_c = A M_c \qquad (9)$$

where M_c is the convective mass flux from the convection scheme and A is a constant of proportionality dependent on the type of convection scheme and differing for land and sea points. (8a) and (8b) are used to distinguish between those cases where low cloud occurs in a generally moist atmosphere in association with a disturbance and those where it occurs as a more persistent feature in association with the tradewind inversion. With convective cloud the assumption is made that if deep

cloud is predicted then only 10% of the convective cloud cover is allowed to occupy the full depth, the remaining 90% being treated as low level shallow convection. This is an attempt to represent the observed situation in a disturbance where, over the area covered by a grid square, only a few isolated cumulonimbus clouds exist in association with an extensive out-flow cirrus shield and a considerable amount of lower level shallow convection.

The model uses a penetrative convection scheme (Lyne and Rowntree 1976) which is based on the idea of an ensemble of buoyant plumes (termed a parcel) of varying characteristics, starting at one level and extending upwards to different heights depending on their characteristics. The initial size of the parcel is determined in part by the instability in the lowest unstable model layer. As the parcel ascends it grows by entrainment provided that the environment is sufficiently unstable that little detrainment is required to maintain buoyancy. The parcel is also modified by latent heat release when it becomes saturated. A maximum parcel size is reached which is dependent on the environmental instability. Beyond that point the parcel maintains buoyancy by detrainment until it reaches a minimum size or the maximum height for an undilute parcel. Since detrainment is generally assumed to occur with zero buoyancy, the heating of the environment occurs mainly through the mass descent which compensates the ascent of the buoyant plumes, although moistening by detrainment and re-evaporation of condensed moisture does compensate, to some extent, for the drying and warming effects of this descent.

The model was integrated for three days from initial data valid at 12Z on 4/9/74. The radiation and cloud schemes were called every two hours of model time. During these two hours the radiative heating rates and cloud amounts remained fixed. In addition to normal model dumps, radiation parameters and cloud amounts were also stored. Data on convective activity such as the parcel sizes and the temperature and moisture increments by convection were also kept.

Two experiments were run to test the sensitivity of the model results to the presence of time-dependent cloudiness. In the first, a fully interactive cloud and radiation scheme was used and in the second, all cloud amounts were set to zero so that only clear sky radiative heating rates and fluxes were used.

3 Results

The cloud amounts predicted by the model in the cloudy experiment for day 3, valid at 12Z on 7/9/74, are shown in figs 6-9 and have been discussed in detail by Walker (1978). In fig. 6, showing the distribution of convective cloud, a distinction has been made between those areas with deep and those with shallow convection. In general the cloud scheme has been reasonably successful in predicting the main features of the cloud field observed for that date.

The inclusion of time-dependent clouds interacting with the radiation field had a considerable effect on the rainfall and synoptic development in the model. Figs. 10 and 11 show the total rainfall accumulated during day 3 for each experiment and Figs. 12 and 13, the winds at level 9, which is approximately 850 mb. The cloudy case shows more development over the sea with increased rainfall whereas over the land the rainfall has decreased and the disturbances are less intense. Over West Africa the clear case has a well-developed vortex whereas the cloudy case shows a generally weaker circulation pattern. In contrast the effect of interactive clouds over the sea has been to intensify somewhat the central Atlantic disturbance and the wave near 50W. Looking farther west to the Caribbean, the cloudy case has developed a closed circulation which is not present in the clear case, suggesting that the interaction between clouds and radiation is capable of producing substantial cyclonic development.

The contrast in the model's response over land and sea to the presence of interactive cloud implies that different mechanisms are operating over each surface type. Over land the response of the model to the presence of cloud can be understood by considering the surface heat balance for which the equation is:

$$C_* \frac{\partial T_*}{\partial t} = R - LE - H \qquad (10)$$

where C_* = surface thermal capacity (20.9 J cm^{-2} K^{-1})

T_* = surface temperature

R = surface radiative flux

LE = evaporation

and H = sensible heat flux

Both LE and H are dependent on the surface temperature through the humidity and temperature gradients between the surface and the lowest model level. R also responds to changes in T_* through the surface infrared cooling. Over land, because C_* is small, the sum of LE and H is strongly governed by the net surface radiative flux. The partitioning of energy between LE and H is determined by the soil moisture content which is kept fixed and is the same for each experiment (Lyne and Rowntree 1976). Clouds affect the surface radiative flux, firstly by reducing the incident solar flux and secondly, by increasing the downward infrared flux. In general the decrease in solar flux far outweighs that in the net upward longwave flux. The net decrease in the surface radiative flux in the cloudy case results in cooler surface temperatures and lower evaporation and sensible heat flux. Over land convective activity is controlled by the upward fluxes of heat and moisture which themselves are determined in part by the surface radiative flux. The lower rainfall in the cloudy case can thus be related to the reduced surface solar flux arising from the presence of clouds. Walker and Rowntree (1977) have shown that, over moist land, disturbances derive their eddy kinetic energy through the baroclinic conversion of eddy available potential energy whose source is latent heat release from convection Thus a decrease in evaporation and surface heating implies a decrease in moist convective activity, less generation of eddy available potential energy and ultimately less eddy kinetic energy. Over land the mechanism by which cloud-modulated radiation affects convective activity appears then to be through changes in the surface radiative flux which result in differences in the upward fluxes of heat and moisture.

Over sea the model's response to clouds is more difficult to interpret. In the model the sea surface temperatures are kept fixed so that over the oceans there is no way in which changes in the surface radiative flux can alter the dynamics of the atmosphere above. Even in reality the large thermal capacity of the oceans means that, over the life-time of synoptic features, they are unlikely to respond to any changes in the net surface radiative flux. Thus the mechanism by which the inclusion of interactive cloud affects the atmospheric dynamics over the oceans must be through changes in the atmospheric radiative heating.

Differences between the two integrations are evident during the first day. It

was decided therefore to choose a limited area on the first day and to study this in detail to see how the differences arose and how they were related to the cloud-induced variations in radiative heating rates. The area chosen covered the GATE B-scale area through which a disturbance passed during 5th September 1974. The rainfall and level 9 winds over this limited area at day 1 are shown in figs. 14 and 15. Already the cloudy case is showing more development and rainfall. Vertical cross-sections of vertical velocity at 12Z, 5/9/74 and total daily mean radiative heating for the period 12Z 4/9/74 to 12Z 5/9/74 along 7N through the centre of the vortex are shown in figs 16 and 17 for each experiment. The clear case shows a uniform cooling of about 1 K/day throughout the troposphere. In contrast the cloudy case shows a large variability in heating rates which can be associated with the distribution of cloudiness shown in fig. 18. (Note that when deep convective cloud is predicted, 90% is treated as shallow cloud and for the purposes of radiation calculations has been included in the low cloud cover). The upper level warming in the region of the disturbance has arisen from the extensive out-flow cirrus shields which are a common feature of tropical disturbances. The assumption that only a small fraction of a grid square is occupied by deep cumulonimbus clouds has meant that high cloud can play a dominant role in determining the radiative heating at upper levels as averaged over the whole grid square. Since their radiating temperature is much lower than the equivalent black body temperature of the up-welling radiation from below, the net effect of these clouds is one of warming, a good example of this being the observed infrared heating rate profile shown in fig. 4 from Fimpel et al (1977). The effect of the variations in heating rates shown in fig. 17 has been to produce much stronger ascent in the centre of the disturbance since the upper level radiative warming results in a distortion of the pressure field such that the convergence into the system is increased. In other words the horizontal gradients in radiative heating force stronger vertical motions than would occur in a clear atmosphere with uniform radiative heating rates.

Yanai et al (1976) have shown that a strong correlation exists between the large-scale vertical motion at higher levels and deep convection. When frequency

distributions of the level of final detrainment of a convective parcel are compared for the clear and cloudy cases (fig. 19) , the effect of the stronger ascent at upper levels in the cloudy case is clearly seen in the greater number of parcels reaching upper tropospheric levels. The mechanism for this increased occurrence of deep clouds is firstly the thermal destabilisation in the upper troposphere caused by adiabatic cooling due to the large-scale ascending motion, and secondly the greater low-level convergence of moisture into the system due to the stronger vertical motions. The variation in low-level convergence induced by horizontal variations in radiative heating rates has been postulated by Gray and Jacobson (1976) as a possible explanation for the observed diurnal variation in oceanic deep cumulus convection.

The effect of interactive clouds on convective activity has been studied briefly by considering daily mean heat and moisture budgets for a point at 7N, 29W in the centre of the disturbance. The apparent heat source (Q_1) and moisture sink (Q_2) for each integration are shown in fig. 20. Both terms are larger than those given in fig. 1 from Yanai et al (1973) which were typical for a rainfall rate of 10 mm day^{-1} the higher rainfall rates (42 and 35 mm day^{-1}) in these calculations would account for the larger moisture sink and heat source. From a study of a heavy rainfall event in the GATE B-scale area Ruprecht (1979) also gives larger values of Q_1 and Q_2 than Yanai et al (1973). The total heating ($Q = Q_1 - Q_2 - Q_R$) by convection is given in fig. 21. The larger lower tropospheric negative values in the cloudy case arise from the greater low level convergence of moisture into the disturbance. The better organisation of the flow when clouds are present has meant that the transfer of heat by convection from the lower to middle and upper troposphere is more efficient than in the clear case. This could have important implications for the meridional transport of heat between the tropics and mid-latitudes since that heat originates largely from convective transports in cloud clusters.

4. Conclusions

The results of experiments with a tropical model which includes an interactive cloud and radiation scheme have shown that the model is very sensitive to the presence of clouds. Over land clouds affect convection by controlling the surface fluxes of heat and moisture whereas over the sea, the vertical circulations induced by the horizontal gradients in atmospheric radiative heating affect convection both by the greater destabilization occurring in areas of increased ascent and by the greater low-level convergence into the system. In particular the upper level radiative warming due to the presence of medium and high clouds in the vicinity of a disturbance appears to be important in increasing ascent at higher levels which in turn increases deep convection.

References

Arakawa, A and Schubert, W H 1974 'Interaction of cumulus cloud ensemble with the large-scale environment. Part I', J.Atm Sci., 31, pp. 674-701

Dopplick, T G 1970 'Global radiative heating of the earth's atmosphere', Rept. No. 24, Planetary Circulation Project, Dept. of Meteorology, M.I.T., 128 pp.

Fimpel, H P, Kuhn, P M and Stearns, L P 1977 'Measurement of infrared irradiances with radiometersondes during GATE from R. V. 'Meteor', 'Meteor' Forsch., Berlin, Reihe B No. 12, pp 23-30.

Gray, W M 1972 'Cumulus convection and large-scale circulations, Part III. Broadscale and mesoscale considerations', Atmos. Sci. Paper 190, Colorado State University, 80 pp.

Gray, W M and Jacobson, R W 1976 'Diurnal variation of deep cumulus convecti Month. Weath. Rev., 105, pp. 1171-1188.

Griffith, K T and Cox, S K 1977 'Infrared radiative properties of tropical cirrus clouds inferred from broadband measurements', Atmos. Sci. Paper 269, Colorado State University, 102 pp.

Lyne, W H and Rowntree, P R 1976 'Development of a convective parameterisati using GATE data', Met O 20 Tech. Note No. II/70, UK Meteorological Office, Bracknell

Lyne, W.H., Rowntree, P.R., Temperton, C and Walker, Julia 1976 'Numerical modelling using GATE data', Met.Mag., 105, pp.261-271.

Ruprecht, E 1979 Proceedings of Workshop on Parameterisation of Cumulus Convection, ECMWF, 23-25 October, 1978.

Walker, Julia 1977 'Interactive cloud and radiation in the 11-layer model. Part I: Radiation Scheme', Met O 20 Tech.Note No.II/91, U.K. Met. Offi Bracknell.

1978 'Interactive cloud and radiation in the 11-layer model. Part II: Cloud scheme', Met O 20 Tech.Note No.II/122, U.K.Met.Office Bracknell.

Walker, Julia and Rowntree, P.R. 1977 'The effect of soil moisture on circulation and rainfall in a tropical model', Q.J.R.M. 103, pp.29-46.

Yanai, M., Esbensen, S and Chu, J.-H. 1973 'Determination of bulk properties of tropical cloud clusters from large-scale heat and moisture budgets', J.Atm.Sci., 30, pp.611-627.

Yanai, M., Chu, J.-H, Stark, T.E. and Nitta, T. 1976 'Response of deep and shallow tropical maritime cumuli to large-scale processes', J.Atm.Sci., 33, pp.976-991.

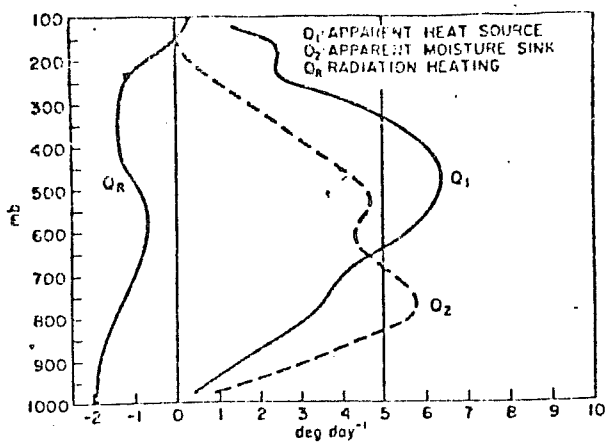

Fig. 1. The mean apparent heat source Q_1 (solid) and moisture sink Q_2 (dashed). The left-hand curve is the radiational heating rate Q_R given by Dopplick (1970) (From Yanai et al 1973).

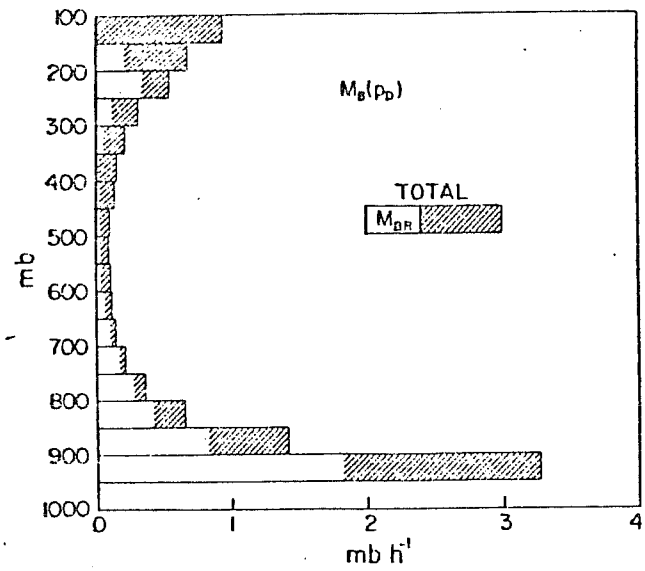

Fig. 2. The mean cloud base mass flux M_B as a function of detrainment pressure P_D. White portion of the bars shows the background mass flux induced by radiative cooling, M_{BR} (From Yanai et al 1976).

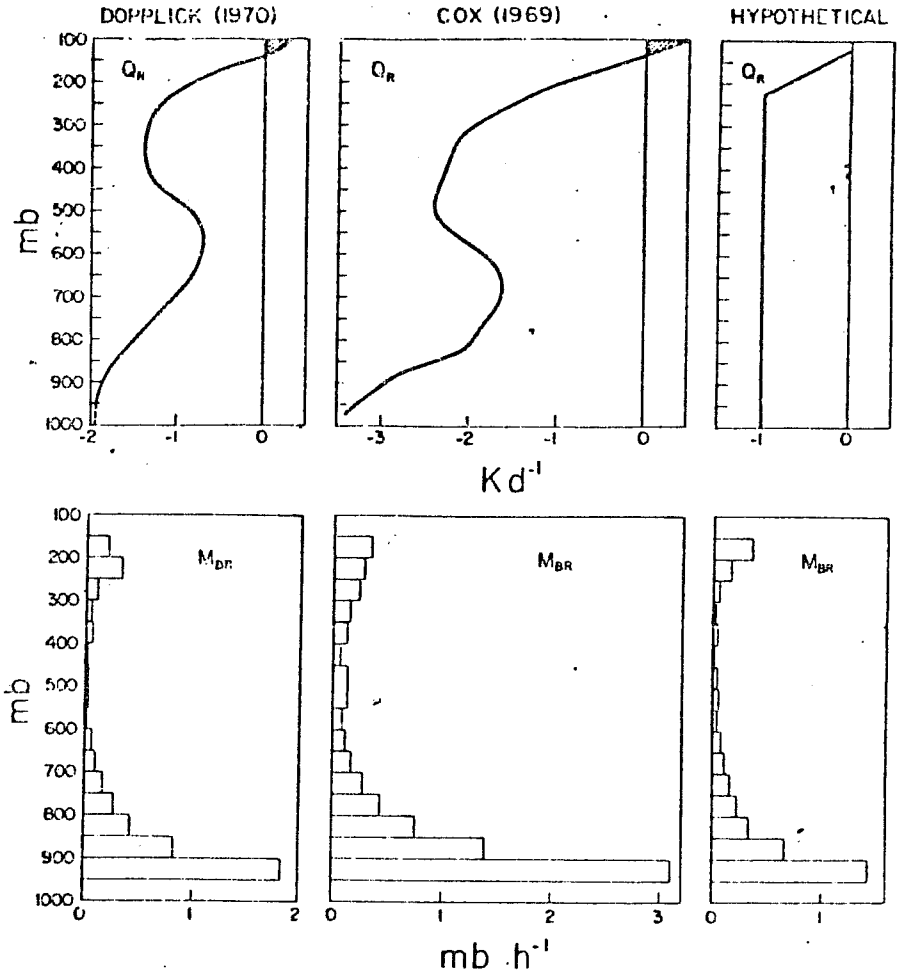

Fig. 3. Three assumed profiles of radiative cooling rates and the corresponding cloud base mass flux M_{BR}. (From Yanai et al 1976).

g. 4. Observed infrared heating rates from GATE (Fimpel, Kuhn and Stearns 1977)

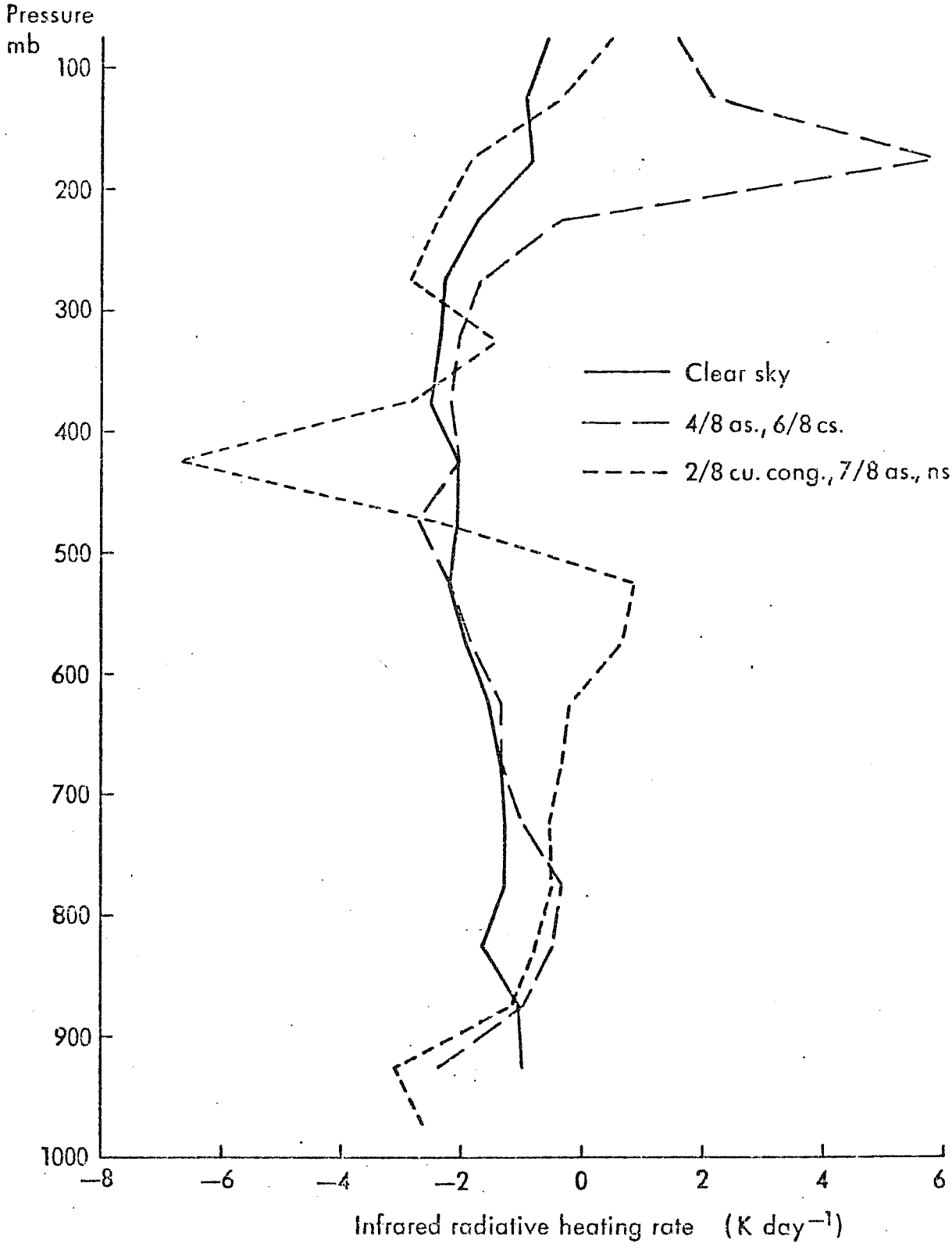

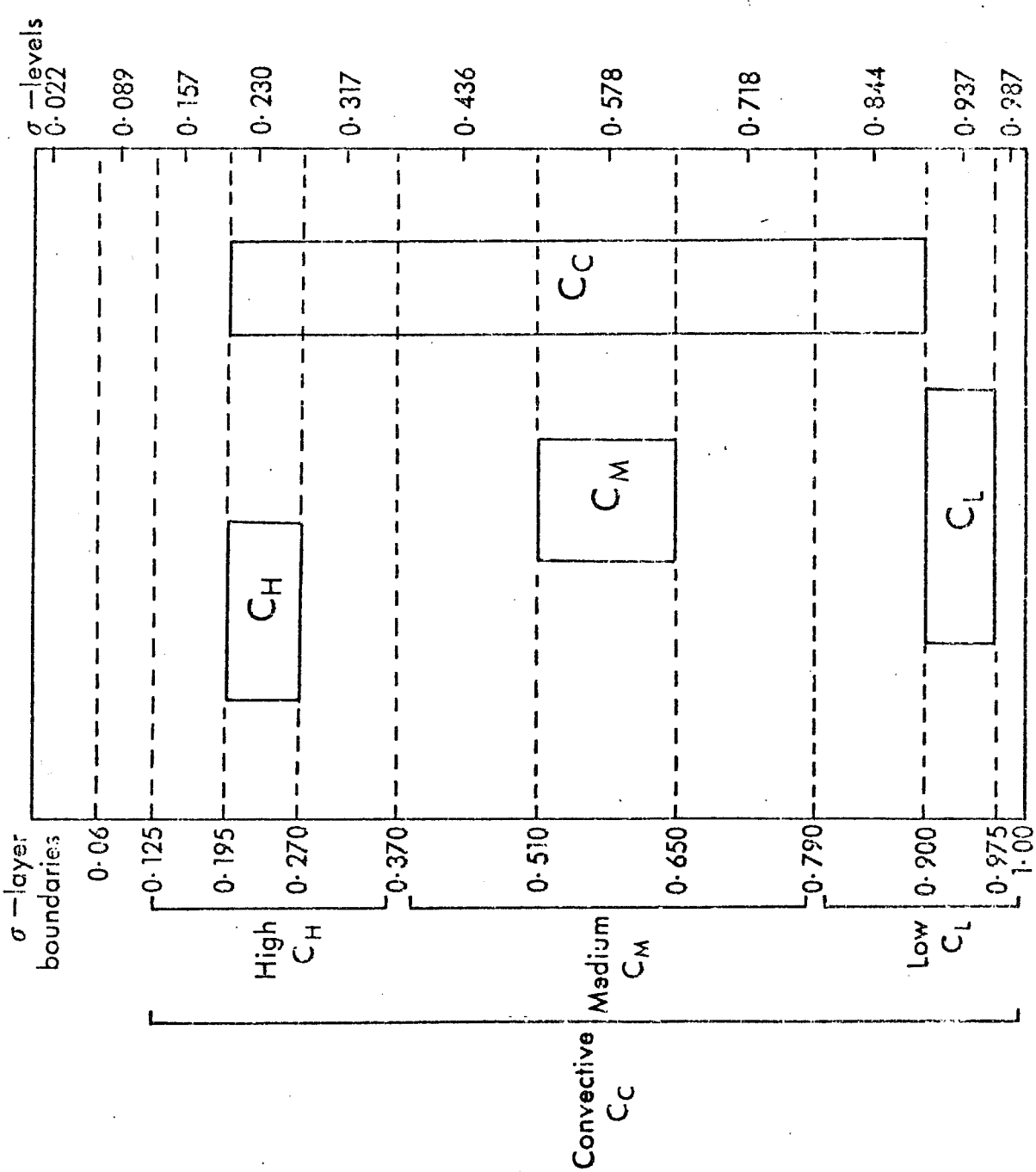

Fig. 5 Distribution of different cloud types over model levels.

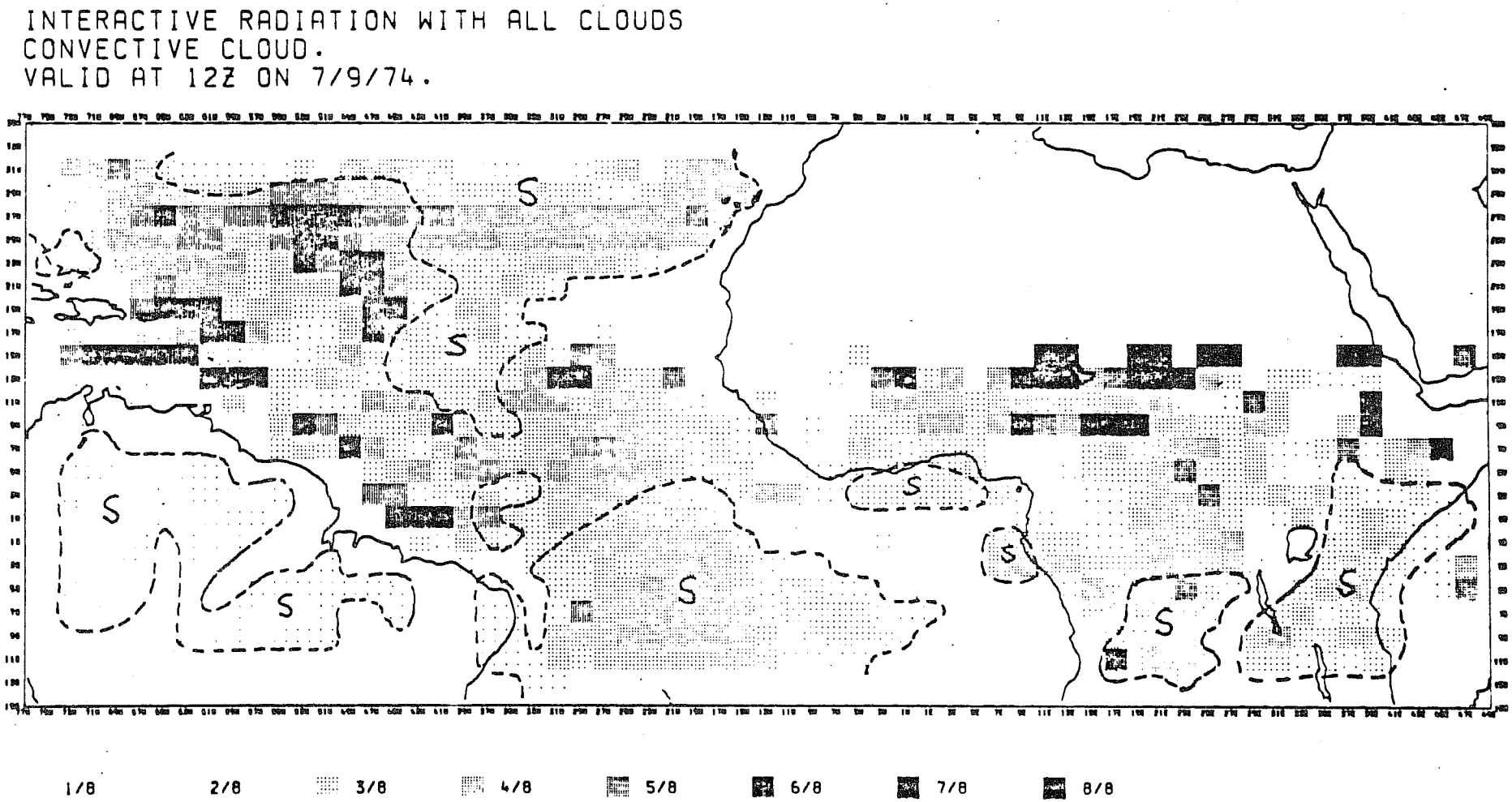

Fig. 6. Predicted distribution of convective cloud at day 3 (S denotes shallow convection; Remaining areas have deep convection).

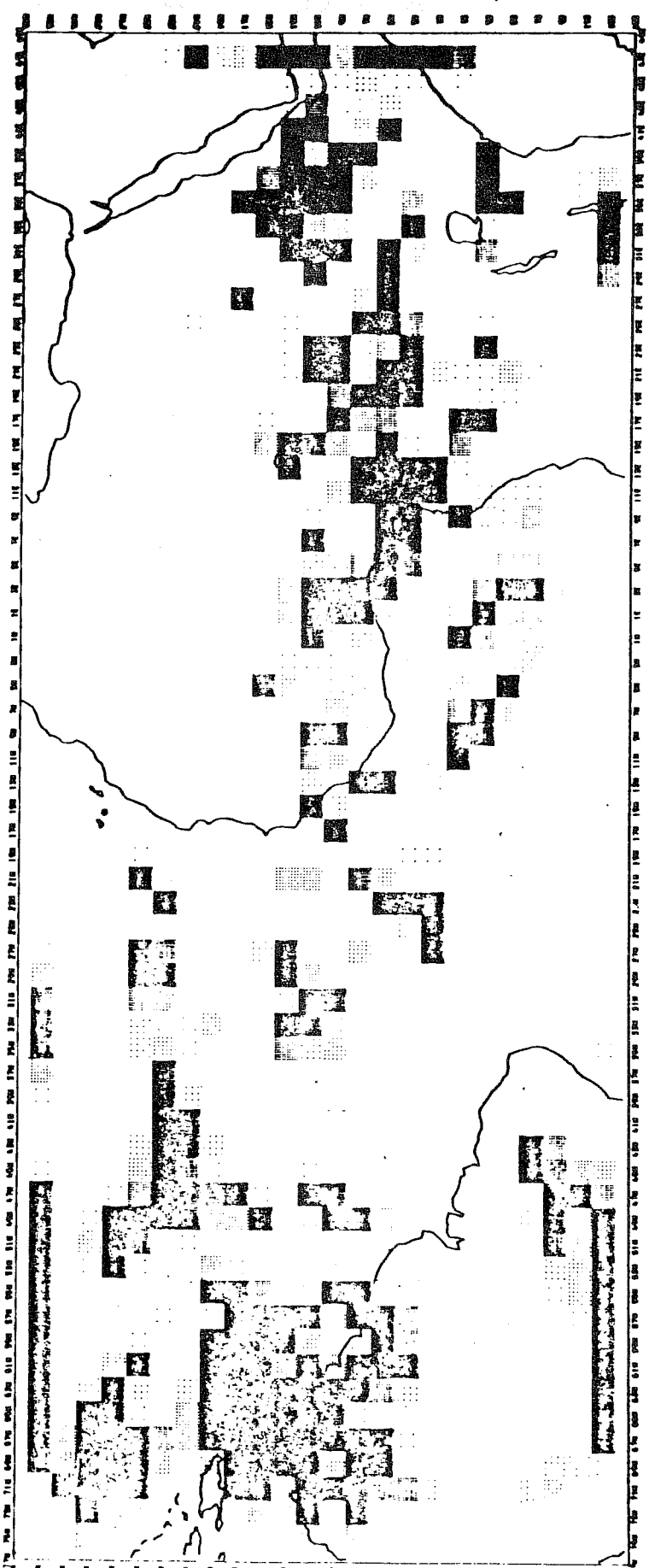

Fig. 7 . Predicted distribution of high cloud at day 3.

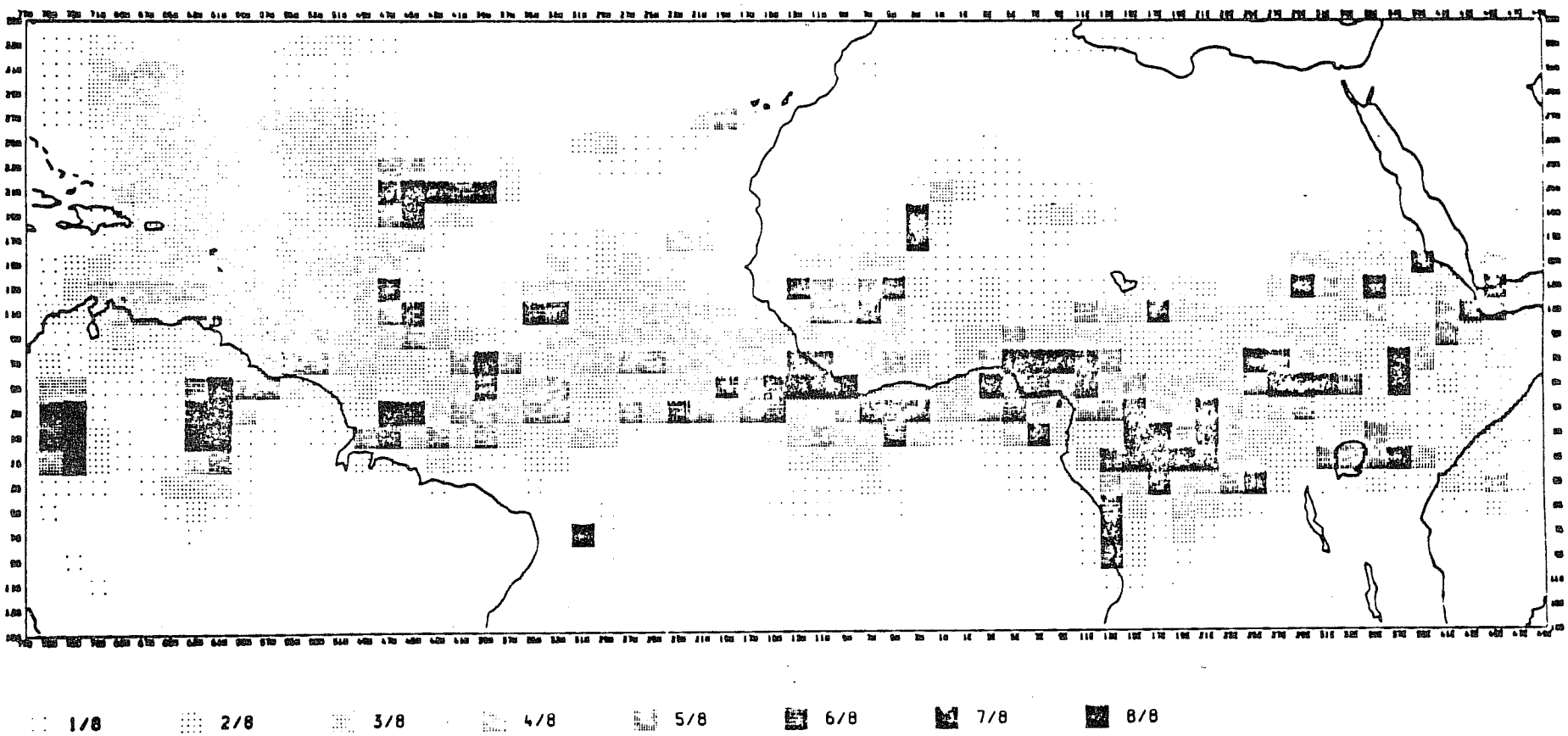

Fig. 8. Predicted distribution of medium cloud at day 3.

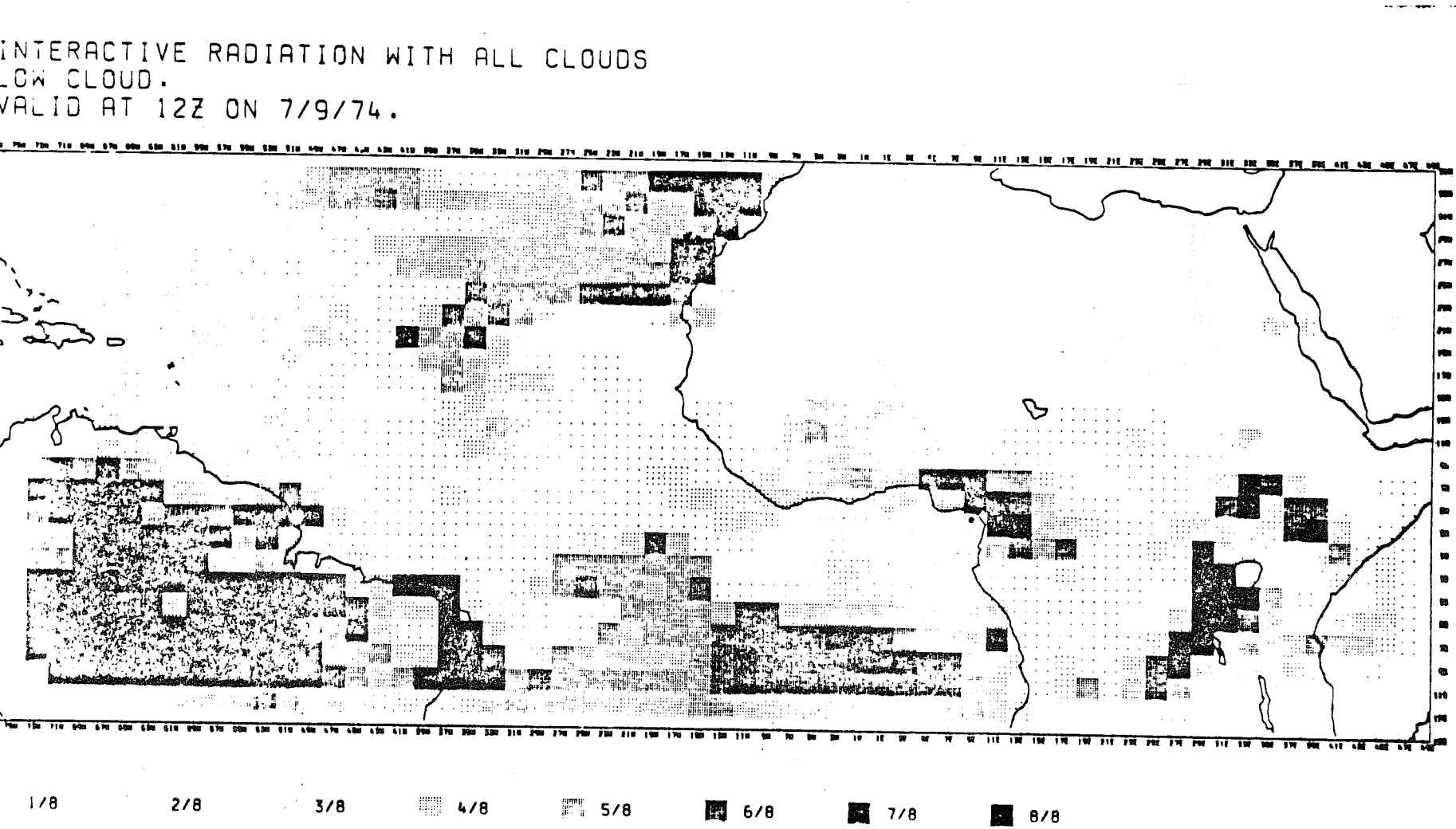

Fig. 9. Predicted distribution of low cloud at day 3.

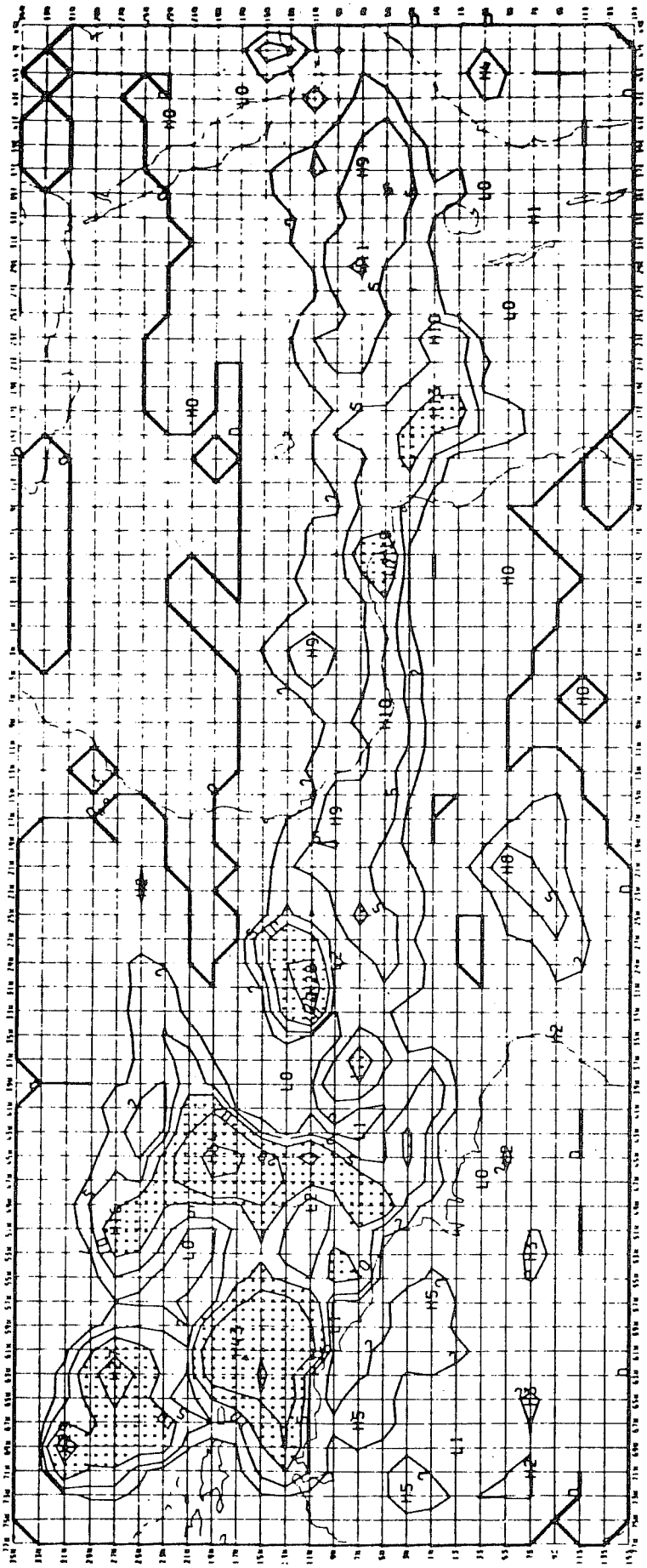

Fig. 10. Accumulated rainfall for day 3 of cloudy case.

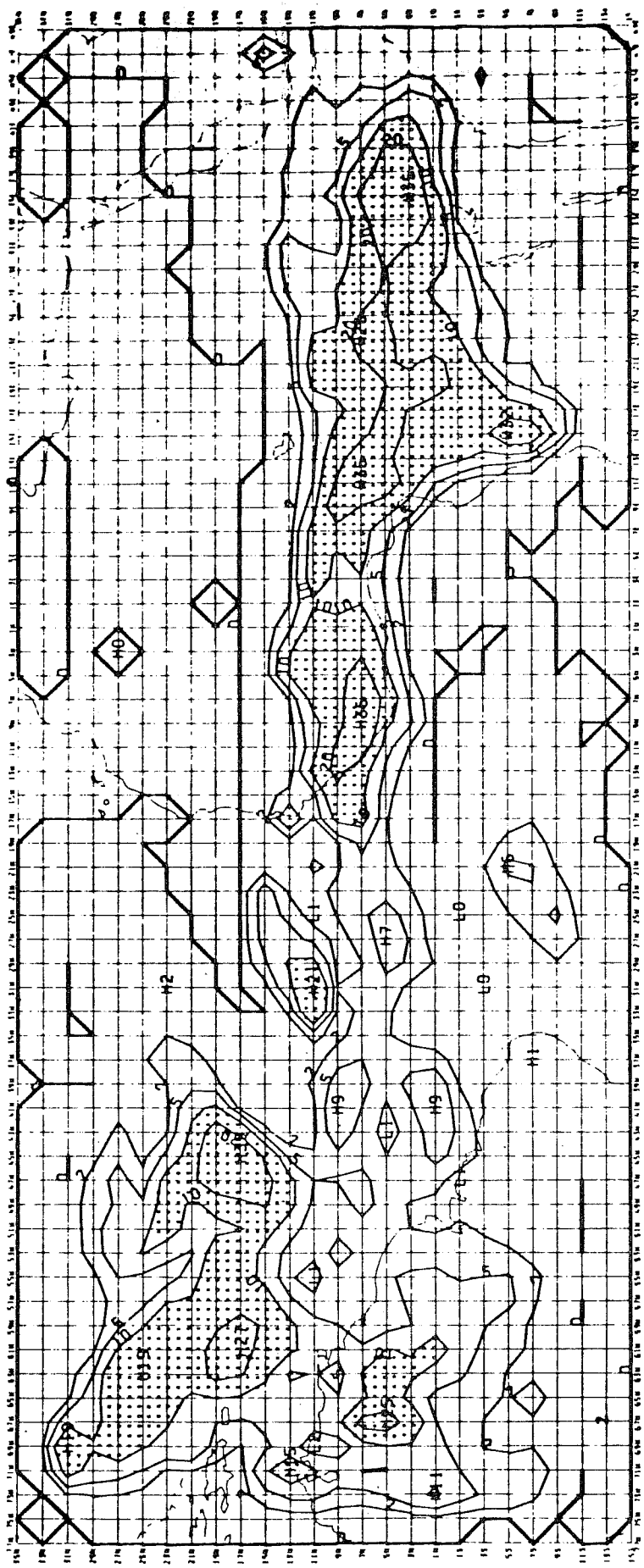

Fig. 11. Accumulated rainfall for day 3 of clear case.

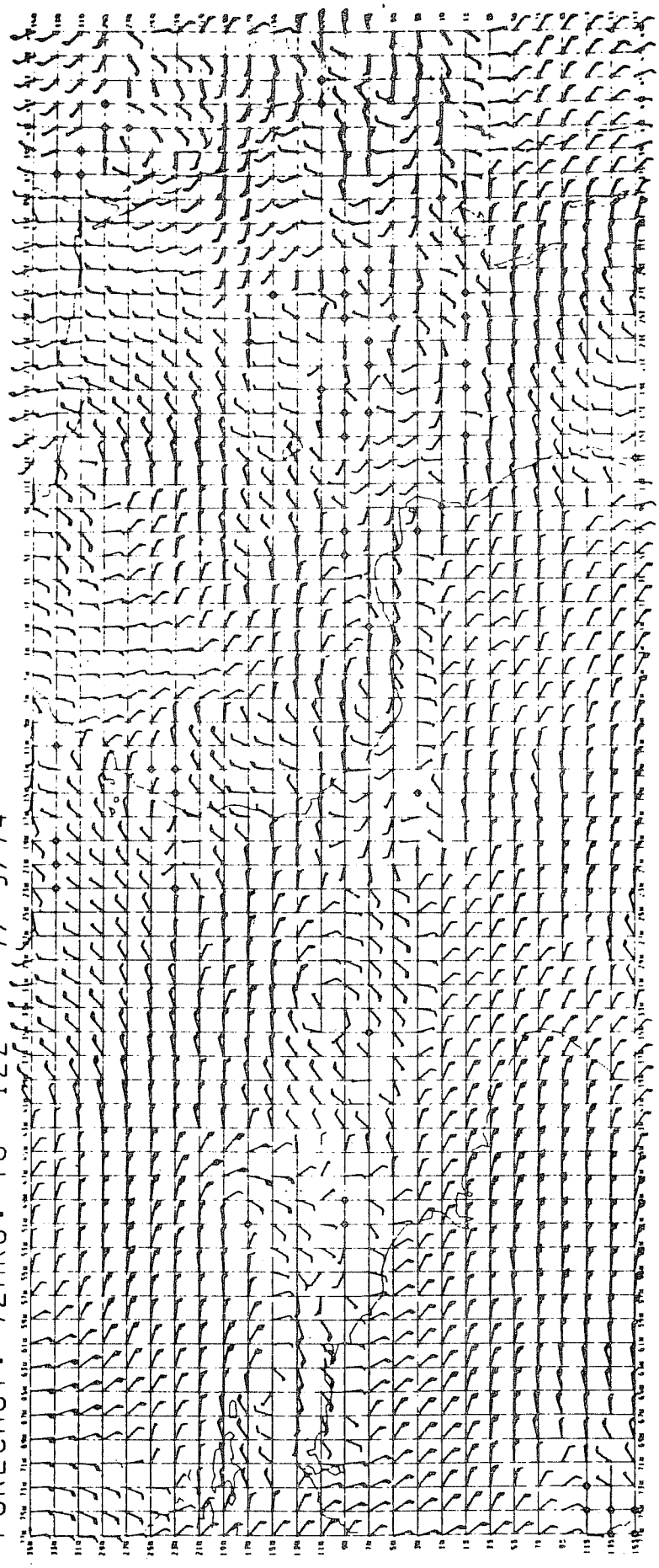

Fig. 12. Winds at level σ = 0.844 for day 3 of cloudy case.

Fig. 13. Winds at level $\bar{\sigma}$ = 0.844 for day 3 of clear case.

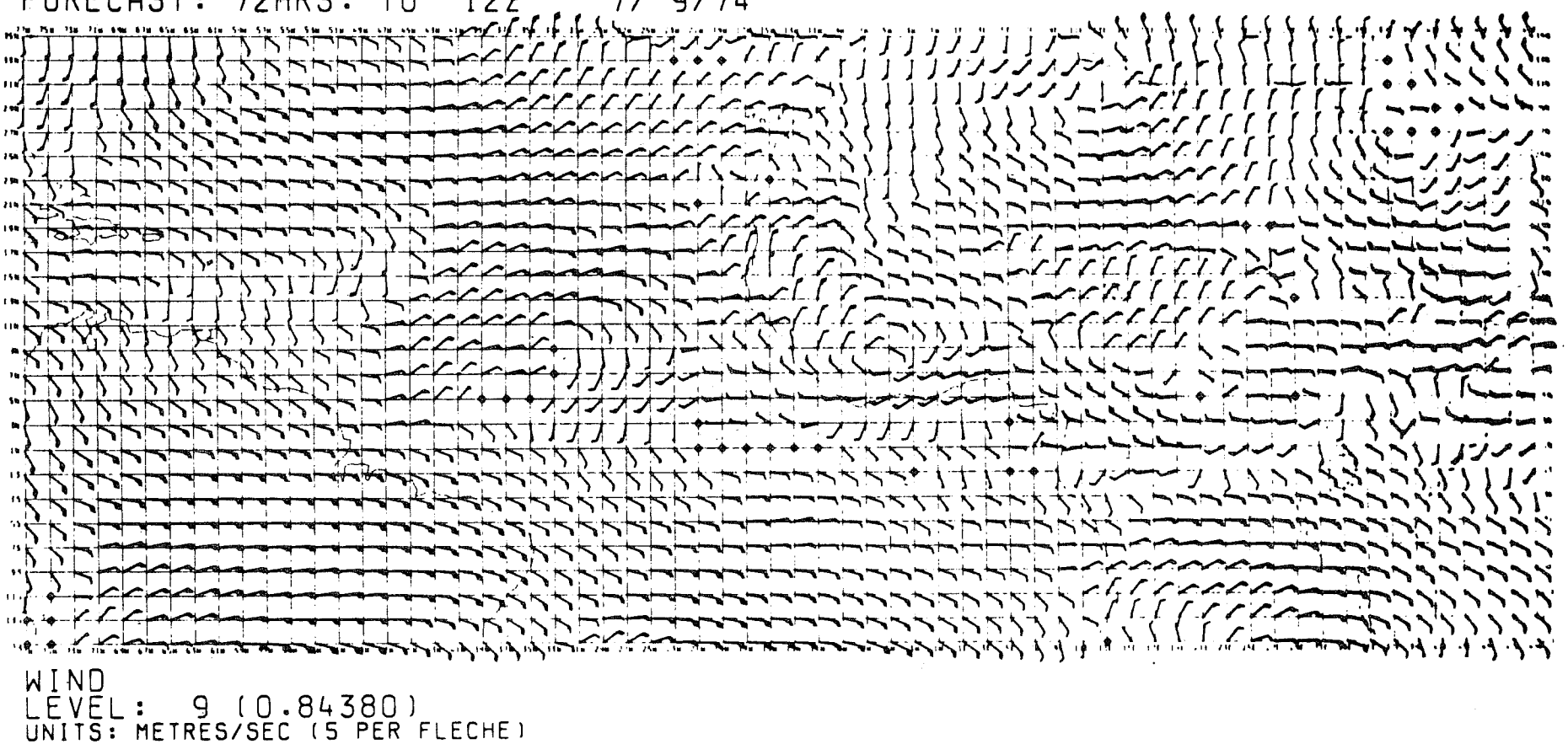

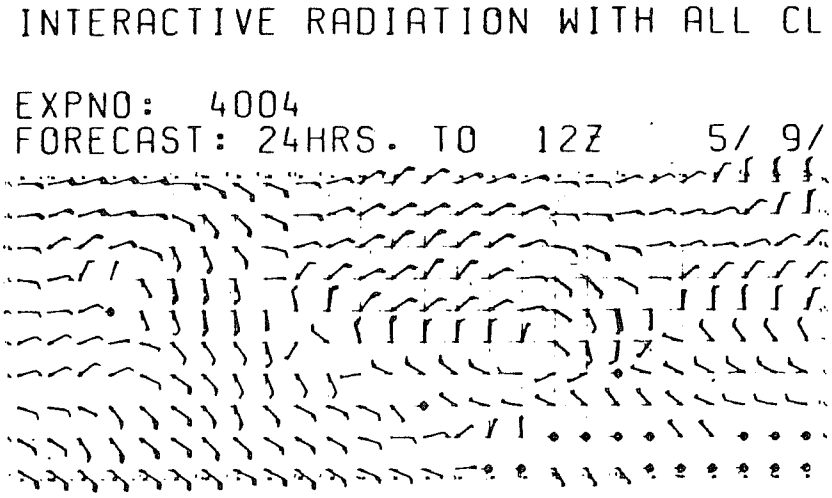

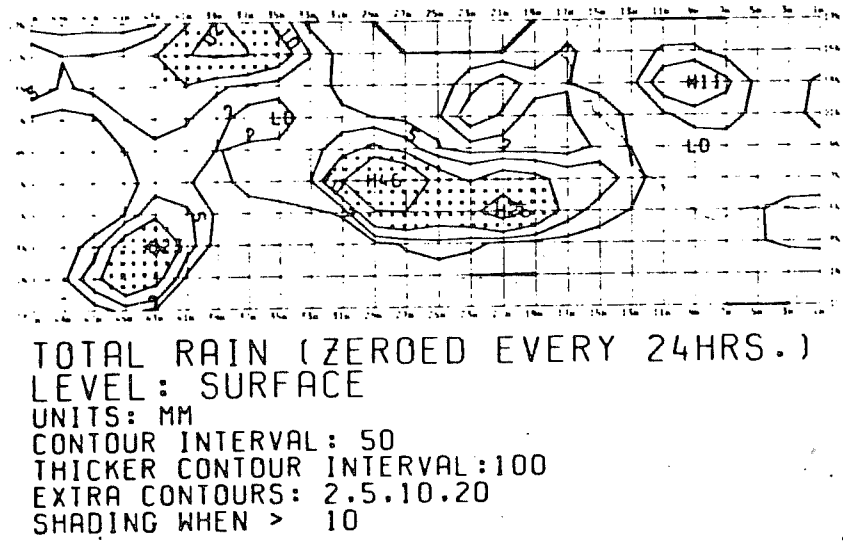

Fig. 14 . Total rain and winds at σ=0.844 for day 1 of the cloudy case for the limited area 17N - 1S, 51W - 1W.

INTERACTIVE RADIATION WITH CLEAR SKIES.

EXPNO: 3000
FORECAST: 24HRS. TO 12Z 5/ 9/74

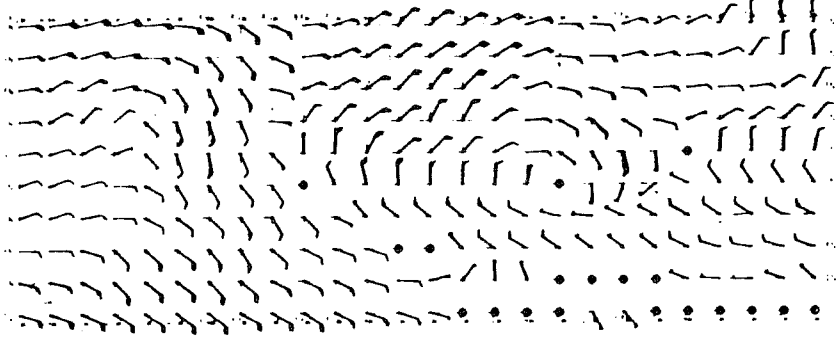

WIND
LEVEL: 9 (0.84380)
UNITS: METRES/SEC (5 PER FLECHE)

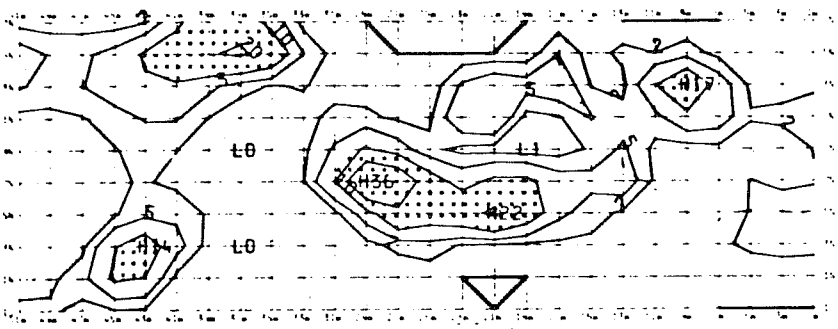

TOTAL RAIN (ZEROED EVERY 24HRS.)
LEVEL: SURFACE
UNITS: MM
CONTOUR INTERVAL: 50
THICKER CONTOUR INTERVAL:100
EXTRA CONTOURS: 2.5.10.20
SHADING WHEN > 10

Fig. 15. Total rain and winds at σ =0.844 for day 1 of the clear case for the limited area 17N - 1S, 51W - 1W.

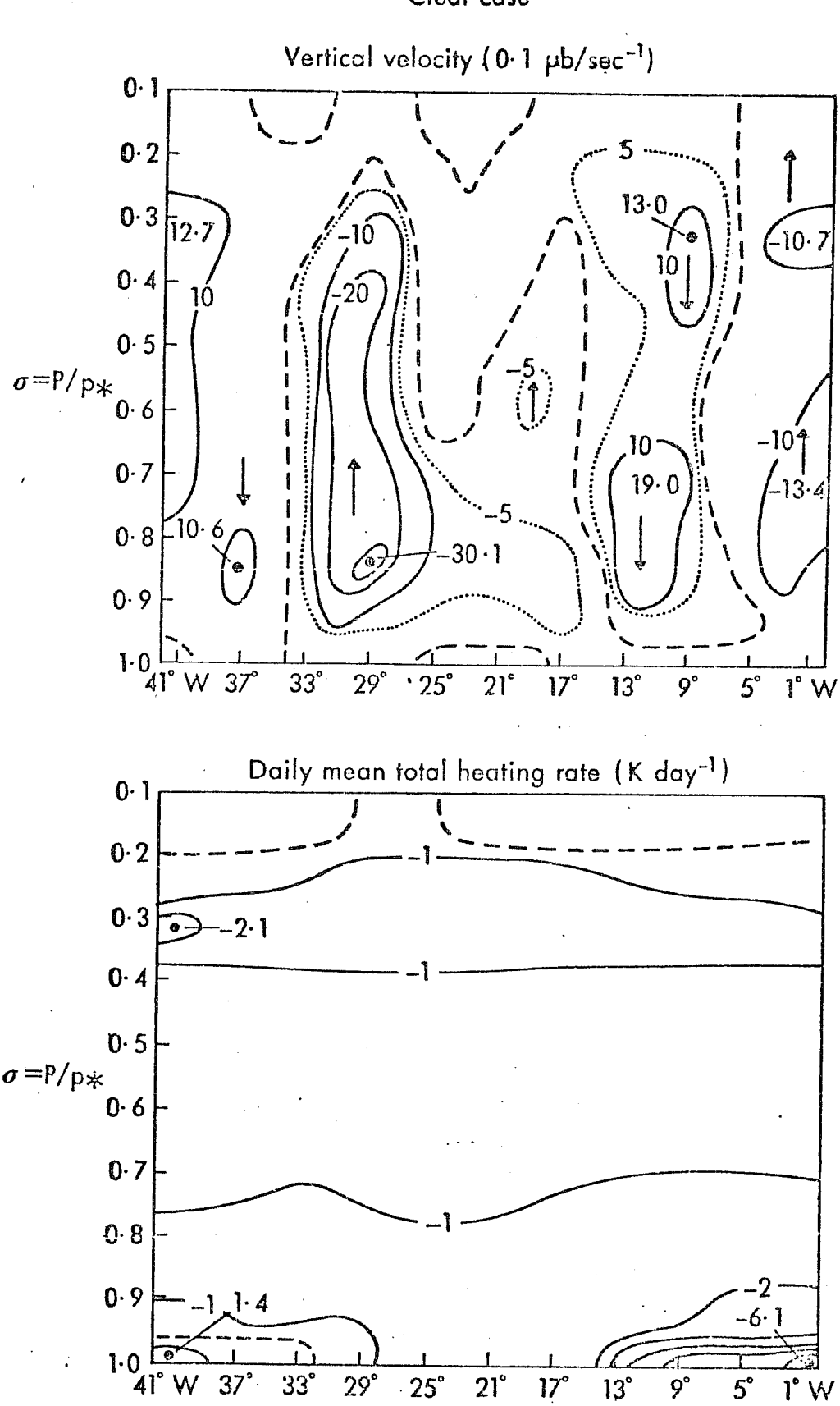

Fig. 16. Vertical cross-section along 7N of vertical velocity and daily mean total radiative heating rate for day 1, clear case.

Cloudy case

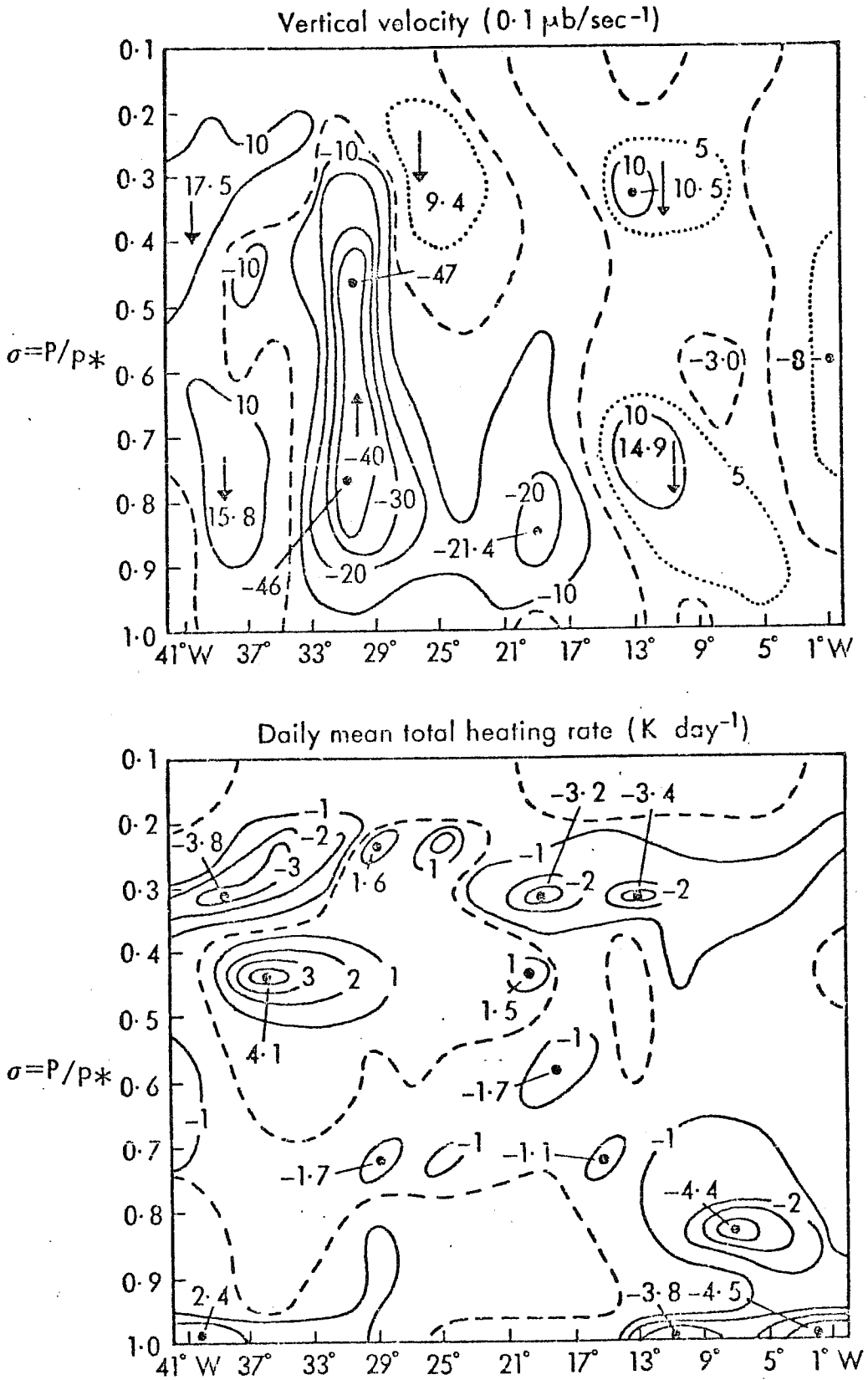

Fig. 17 . As Fig. 16 but for cloudy case.

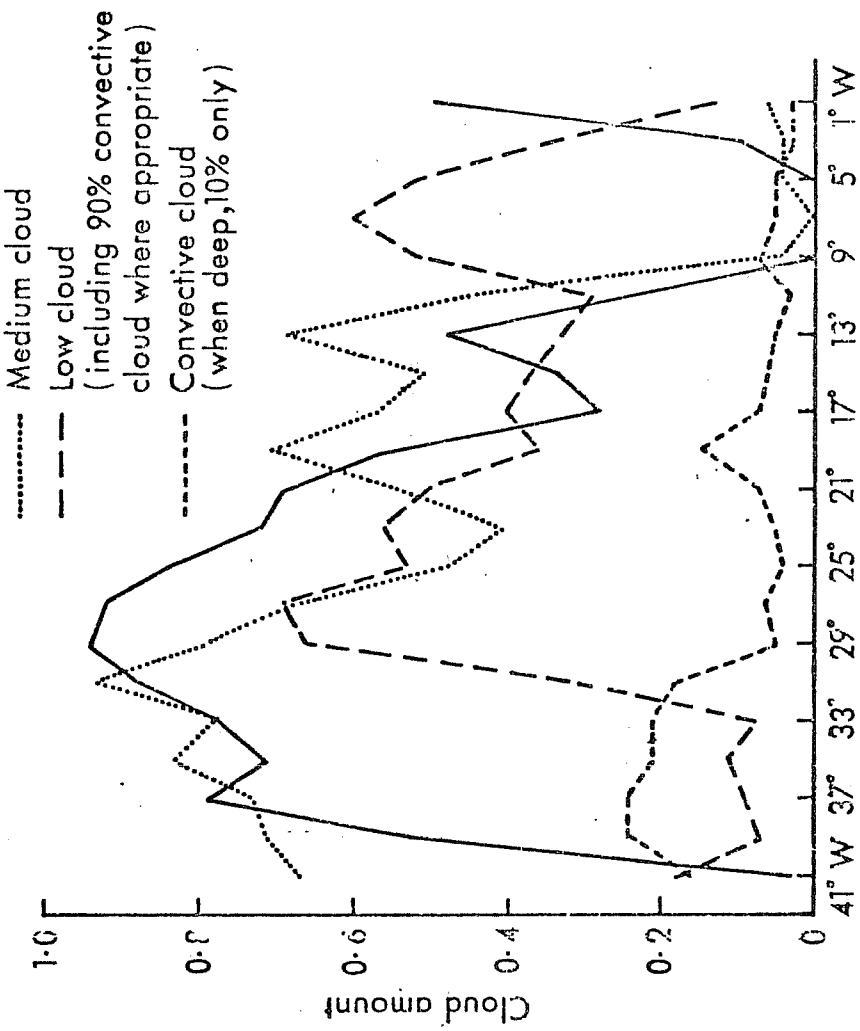

Fig. 18. Daily mean cloud amounts for day 1 along latitude $7^{o}N$

Fig. 19. Frequency distribution of level of total detrainment for day 1 for area 17° N to 1° S, 51° W to 1° W

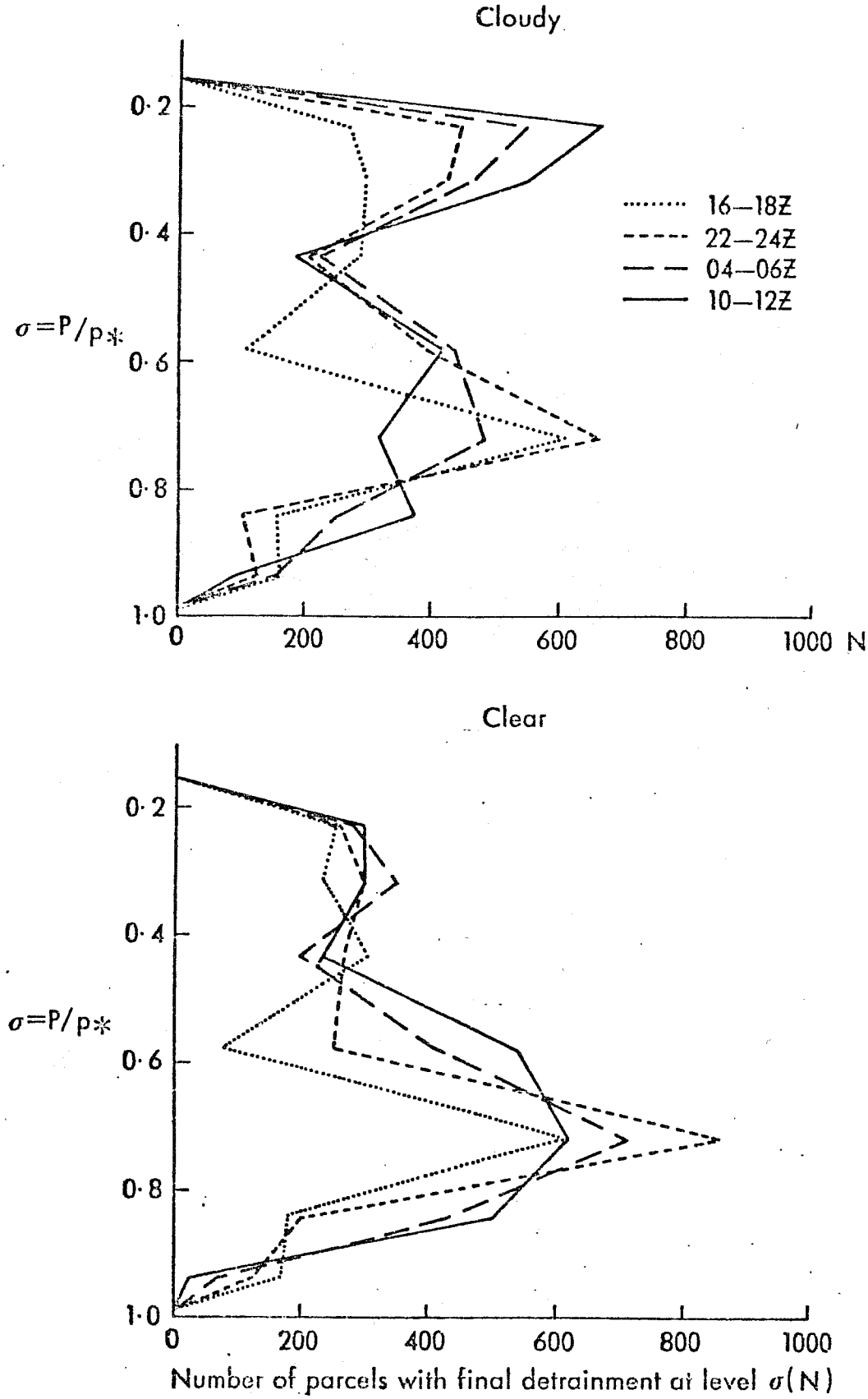

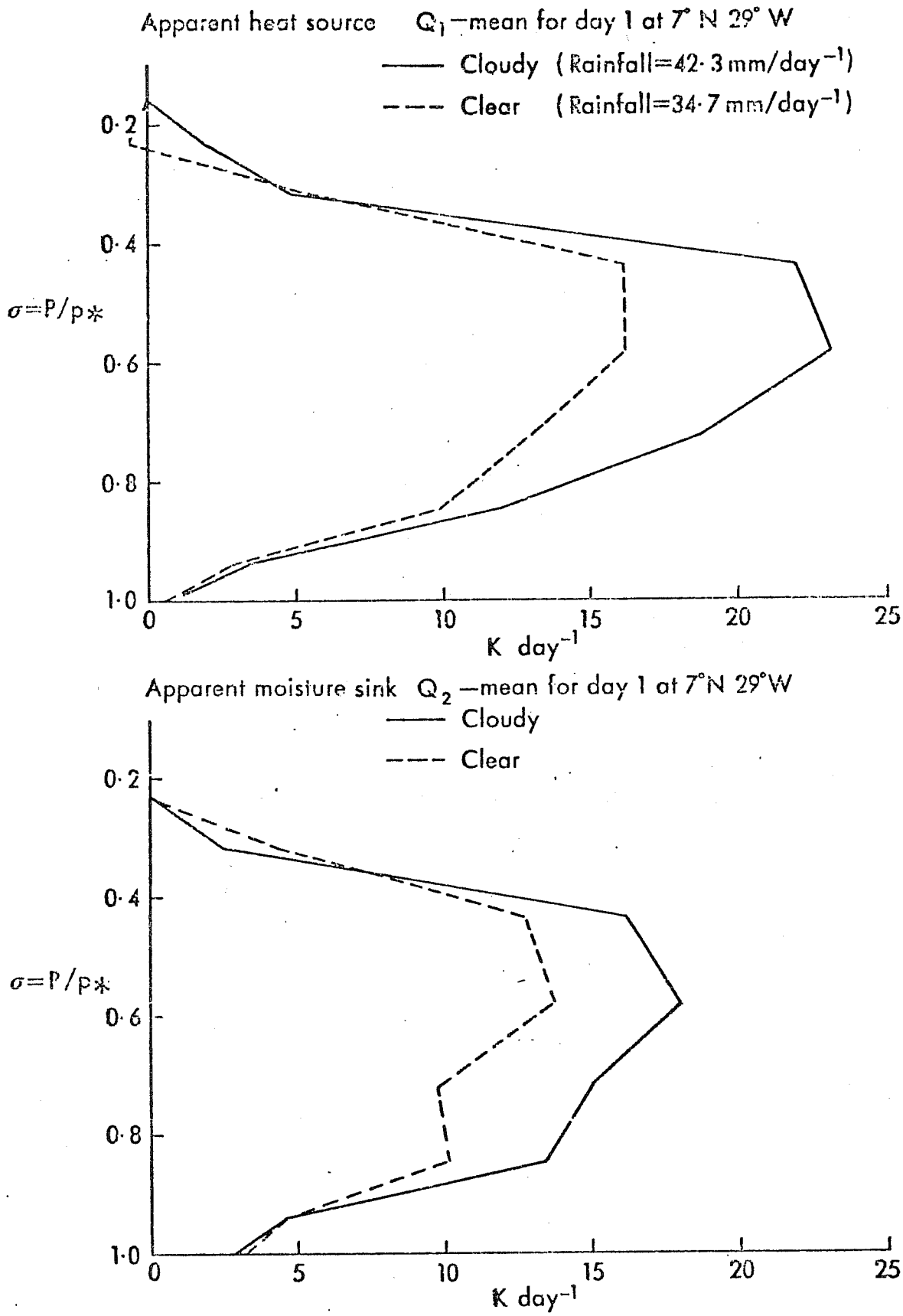

Fig. 20. Apparent heat source Q_1 and moisture sink Q_2 for day 1 at 7N 29W.

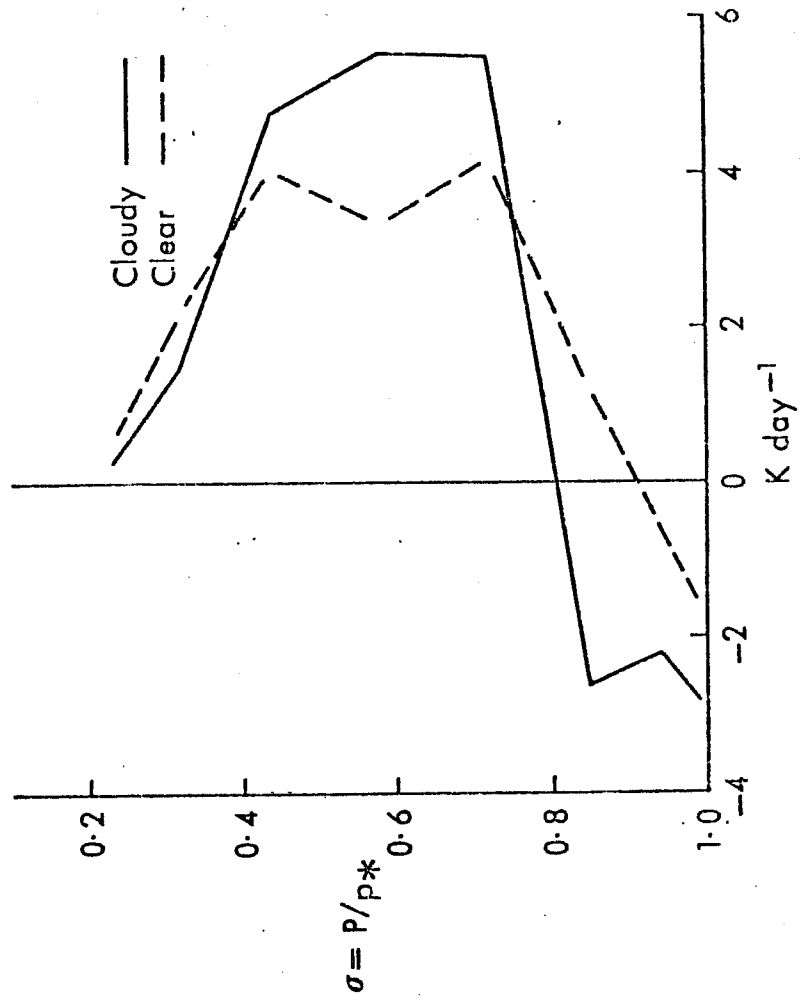

Fig. 21. Apparent heat source $Q = Q_1 - Q_c - Q_R$

Mean for day 1 at 7° N 29°W

REFERENCES

A rather complete list of references on parameterization of cumulus convection until 1977 can be found in Bates' lecture on Cumulus Convection at ECMWF in 1977 (ECMWF, Seminars (1977), pp. 211-229).

References referred to in this paper:-

ANTHES, R.A.,	1977	M.W.R., vol.105, 270-286
ARAKAWA, A.,	1968	Proc. WMO/IUGG Symposium, Tokyo
ARAKAWA, A. and SCHUBERT, W.H.	1974	J.A.S., 31, 674-701
BETTS, A.K.	1973	Q.J.R.Met.Soc.,99, 178-196
BETTS, A.K., GROVER, R.W., and MONCRIEFF, M.W.	1976	Q.J.R.Met.Soc.,102, 395-404
BENISTON, M.G.	1977	Conf. on Hurricanes and Tropical Meteorology, Miami
BREUCH, M.A.E. and RUPRECHT, E.	1977	Meteor. Forschungsergebnisse Ber.,12, 31-41
CESELSKI, B.F.	1974	J.A.S., 31, 1241-1255
CORBY, G.A. et al.	1977	Met. in Comp. Phys., 17
CORBY, G.A. et al.	1972	Q.J.R.Met.Soc., 98, 809-832
CHO, H.R.	1977	J.A.S.,34, 87-97
EMMIT, E.P.	1978	J.A.S.,35, 1485-1502
ELSBERRY, R.L. and HARRISON, E.J.	1972	J.Appl.Met.,11, 255-267
FRAEDRICH, K.	1974	J.A.S.,31, 1838-1849
FRAEDRICH, K.	1976	J.A.S.,33, 262-268

REFERENCES (contd.)

FRAEDRICH, K.	1977	J.A.S.,34, 335-343
GRAY, W.M. and JACOBSON, R.W.	1977	M.W.R.,105, 1171-1188
JOHNSON, R.H.	1976	J.A.S.,33, 1890-1910
JOHNSON, R.H.	1978	J.A.S.,35, 484-494
KREITZBERG, C.W. and PERKEY, D.J.	1976	J.A.S.,33, 456-475
KRISHNAMURTI, T.N. et al	1976	J.Met.Soc.,Japan, 54, 208-225
KRISHNAMURTI, T.N. et al	1978	FSU Rep. No.77-7, Florida State University
KUO, H.L.	1965	J.A.S.,22, 40-63
KUO, H.L.	1974	J.A.S.,31, 1232-1240
LOPEZ, R.E.	1976	M.W.R.,104, 268-283
LORD, S.	1978	Dissertation, University of California
LYNE, W.H. and ROWNTREE, P.R.	1976	Met.O.20, Technical Note No.11/70, Bracknell, U.K
MANABE, S. et al.	1965	M.W.R.,93, 769-798
MANSFIELD, D.A.	1977	Q.J.R.Met.Soc.,103, 569-57
MILLER, M.J.	1978	Q.J.R.Met.Soc.,104, 351-36
MILLER, M.J. and BETTS, A.K.	1977	M.W.R.,105, 833-848

REFERENCES (contd.)

MONCRIEFF, M.W.	1978	Q.J.R.Met.Soc.,104,543-567
MONCRIEFF, M.W. and MILLER, M.J.	1976	Q.J.R.Met.Soc.,102,395-404
MIYAKODA, K. and SIRUTIS, J.	1977	Beitr. z. Phys. d. Atm.,50, 445-486
NITTA, J.	1977	J.A.S., 34, 1163-1186
OOYAMA, K.	1971	J.Met.Soc., Japan, 49, 744-756
OGURA, Y. and CHO, H.R.	1973	J.A.S., 30, 1276-1286
CHO, H.R. and OGURA, Y.	1974	J.A.S., 31, 2058-2065
OKLAND, H.	1977	Institutt for Geofysikk, Oslo, Rep. No.26
O'BRIEN, J.R.	1970	J. Appl. Met.,9,197-203
REED, R.J. and RECKER, E.E.	1971	J.A.S., 28, 1117-1133
ROWNTREE, P.R.	1973	Met.O 20, Bracknell (Internal script)
ROSENTHAL, S.L.	1978	J.A.S., 35, 258-271
SMAGORINSKY, J. et al.	1965	M.W.R., 93, 727-768
SOMERVILLE et al.	1974	J.A.S., 31, 84-117
SOMMERIA, G.	1976	J.A.S., 33, 216-241

REFERENCES (contd.)

SOMMERIA, G. and DEARDORFF, J.W.	1977	J.A.S., 34, 344-355
THOMPSON et al.	1978	J.A.S. to be published
YANAI, M. et al.	1973	J.A.S., 30, 611-627

EUROPEAN CENTRE FOR MEDIUM RANGE WEATHER FORECASTS

Research Department

Workshops

Nov. 1977	Workshop on the use of Empirical Orthogonal functions in Meteorology
Oct. 1978	Workshop on the parameterization of Cumulus Convection

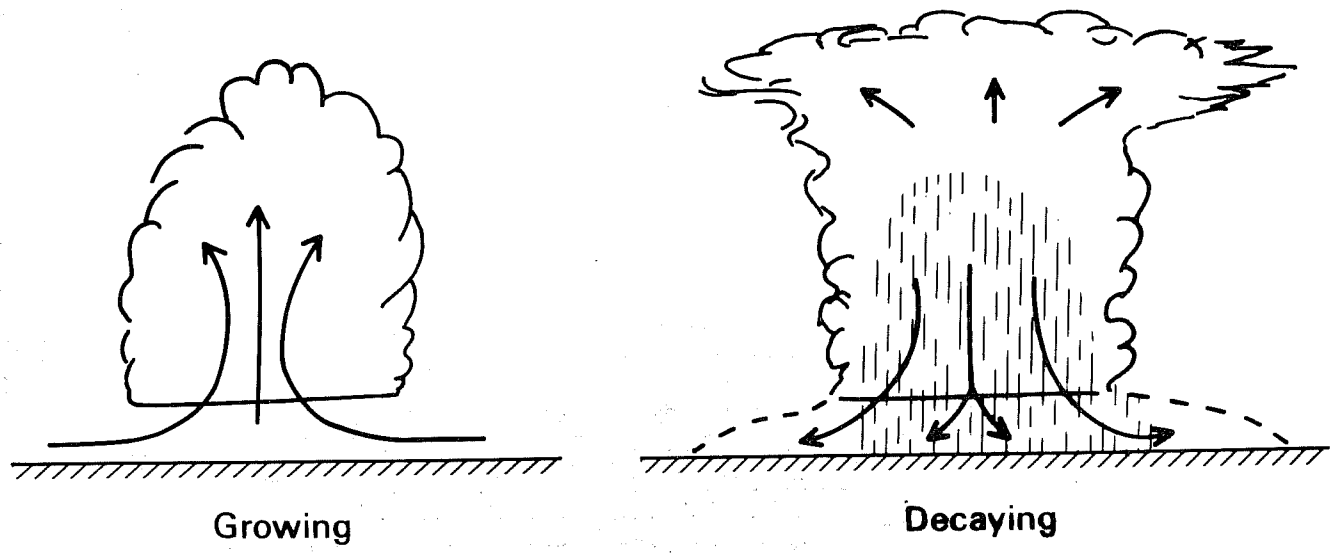

Fig. 1a Schema of a cumulonimbus in small wind shear, typical of summer showers or 'heat' storms over land. Transient with a lifetime < 1 hour. Slow-moving.

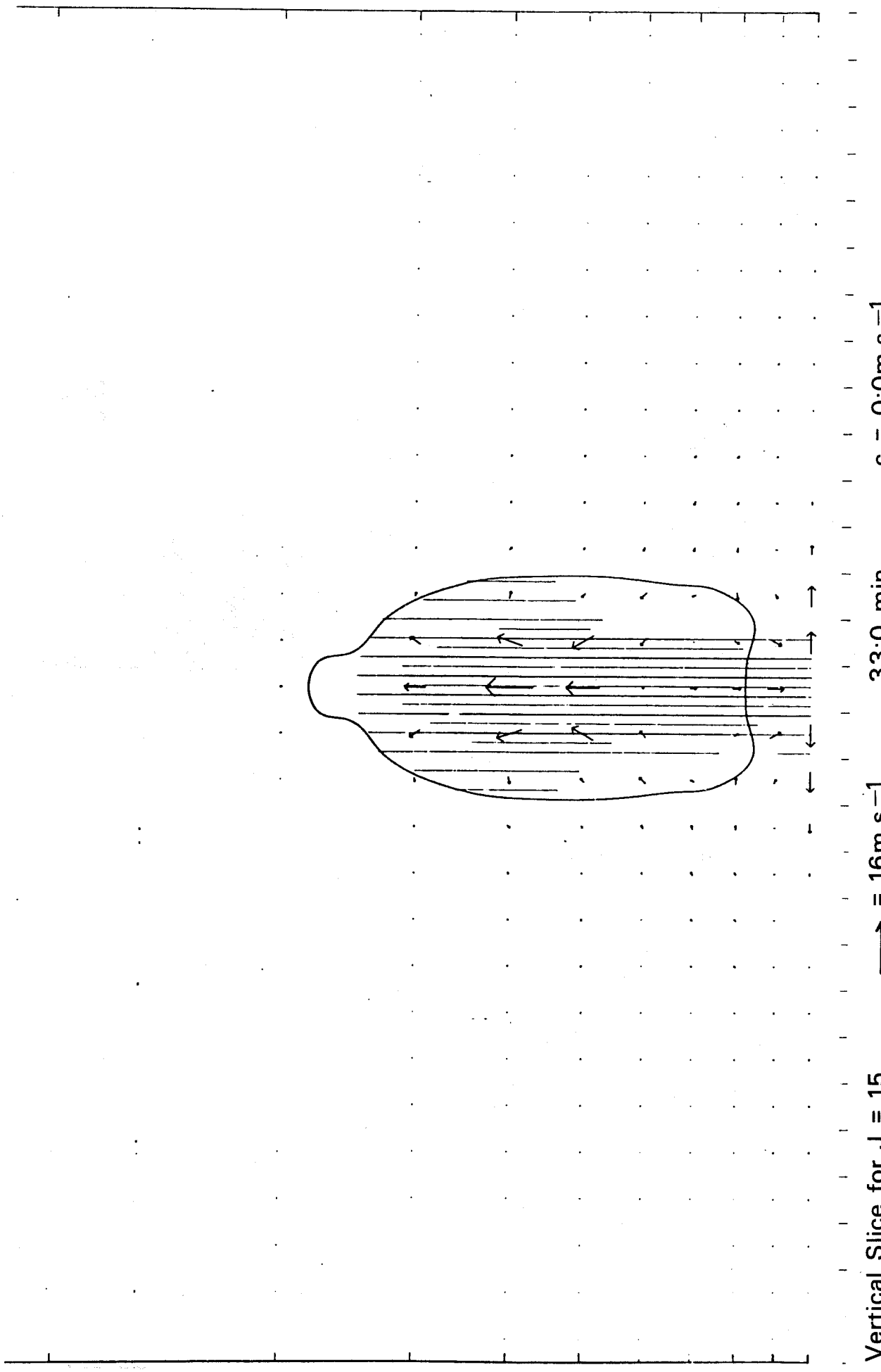

Fig. 1b Corresponding simulation in zero vertical windshear. A vertical slice through the centre of the cloud showing contours of cloud outline, rainwater as vertical hatching, and velocities as arrows.

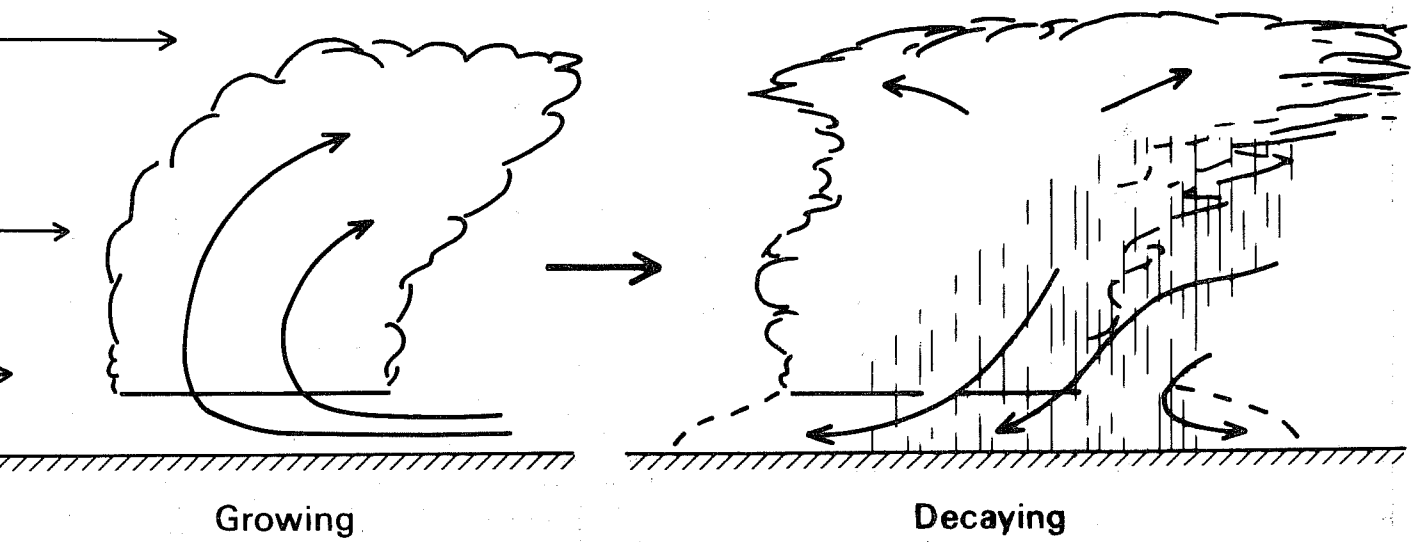

ig. 2a Schema of the relative flow in a cumulonimbus in large, essentially one-directional, windshear typical of showery maritime air, but can be a component of more severe storms. Usually transient and moves with about the mean wind speed.

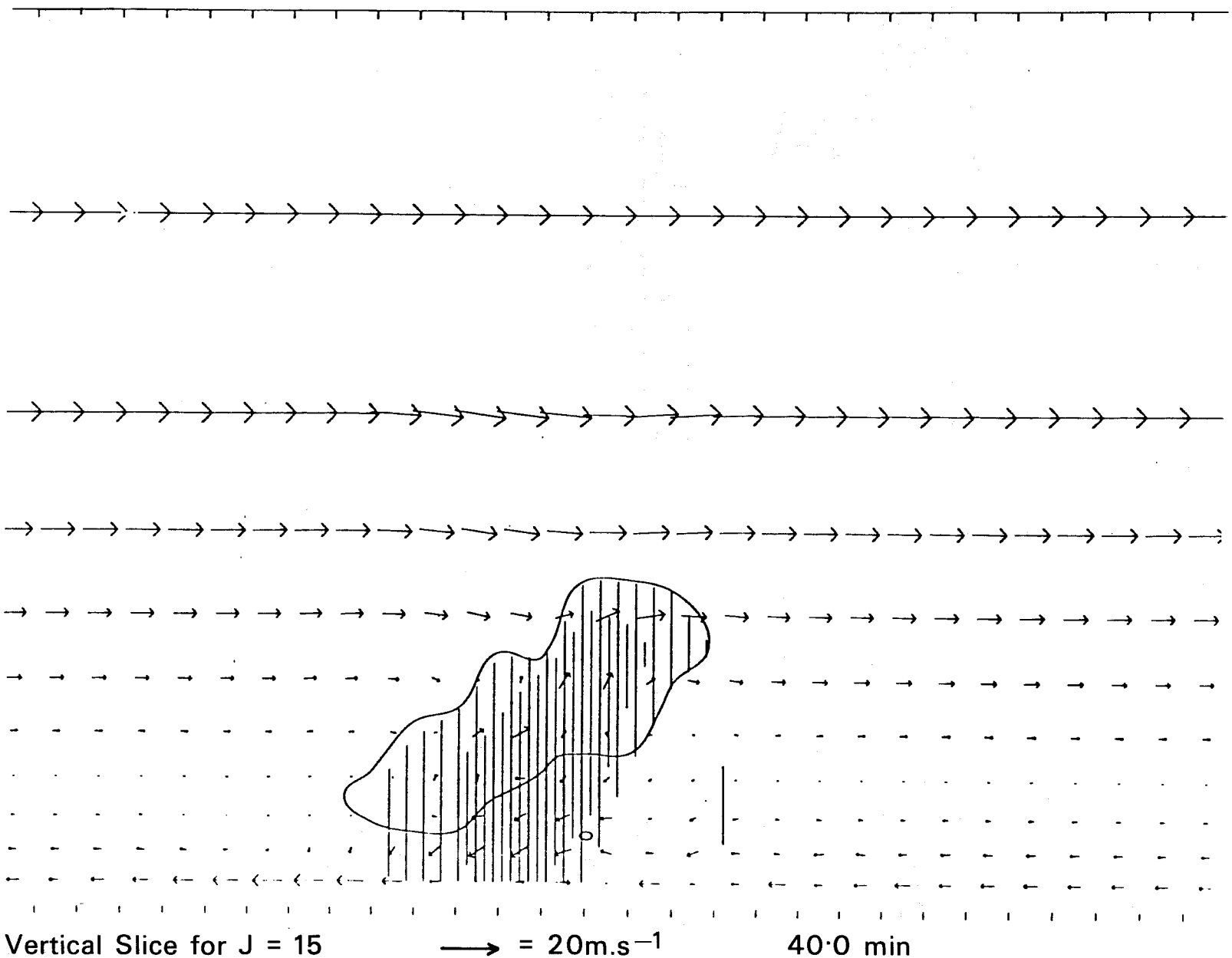

Fig. 2b Corresponding simulation showing the large downshear slope of the cloud and associated updraughts and downdraughts.

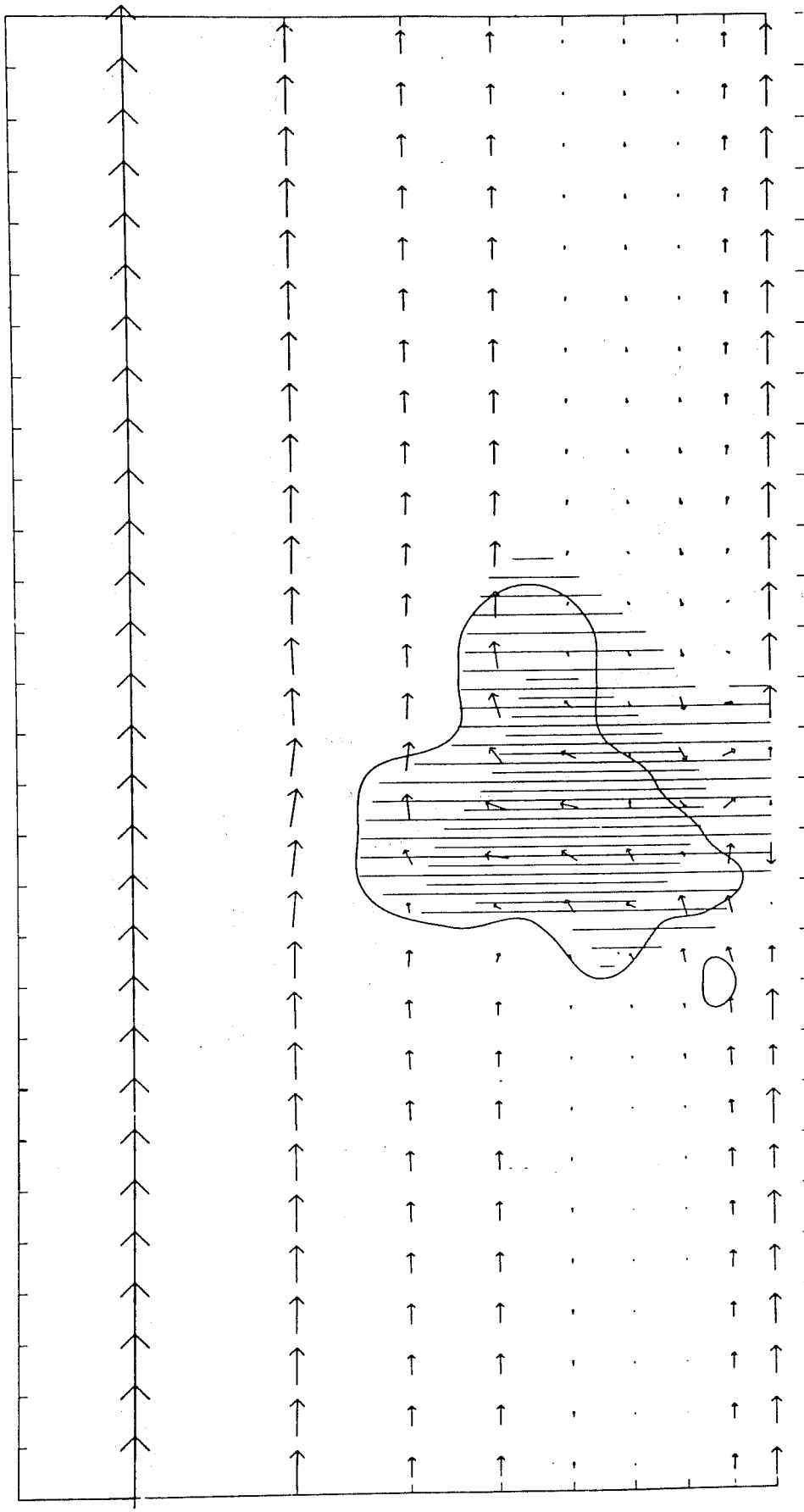

Fig. 3a Vertical slice through simulation of a tropical squall-line showing flow approaching the storm at all levels from one side and exiting from the opposite side.

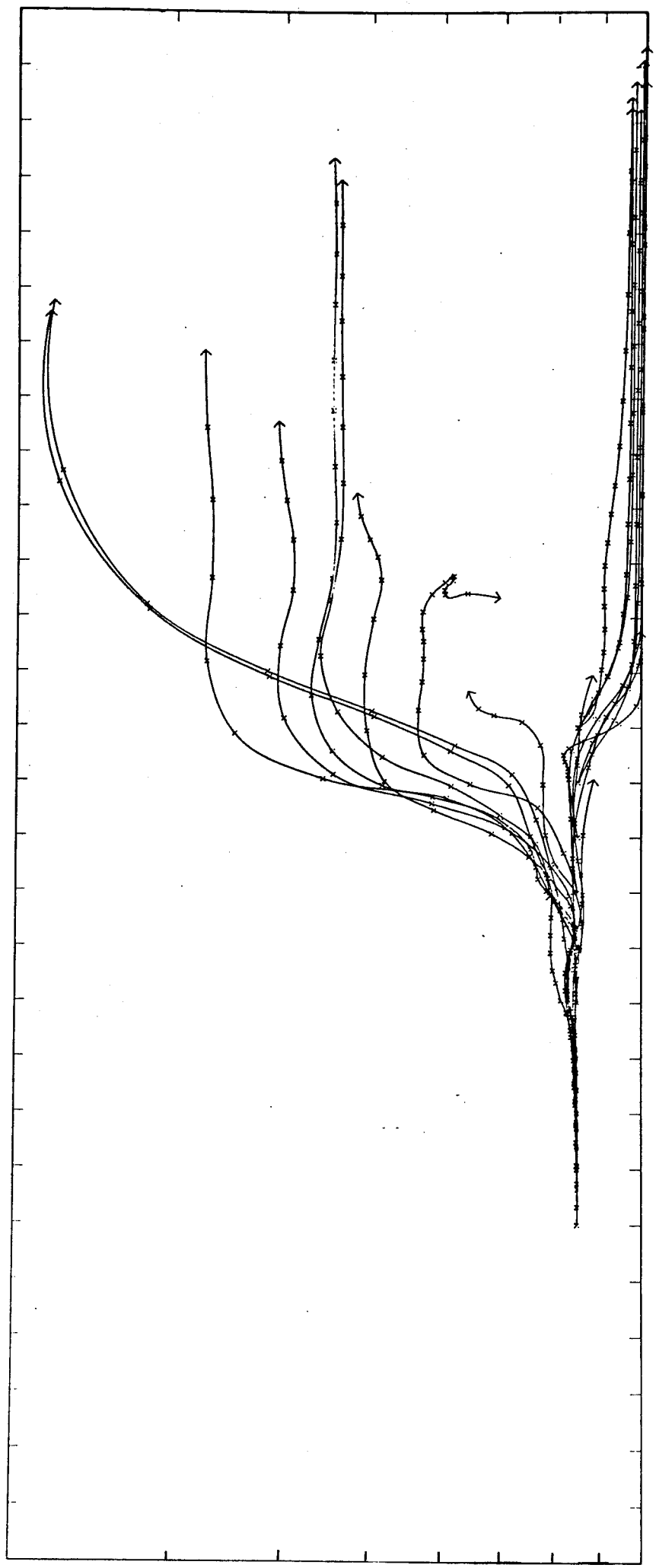

Fig. 3b Trajectories computed from the tropical squall-line simulation showing the distinctive updraught/downdraught structure. Note that trajectories drawn are a projection on the vertical plane and are really three-dimensional

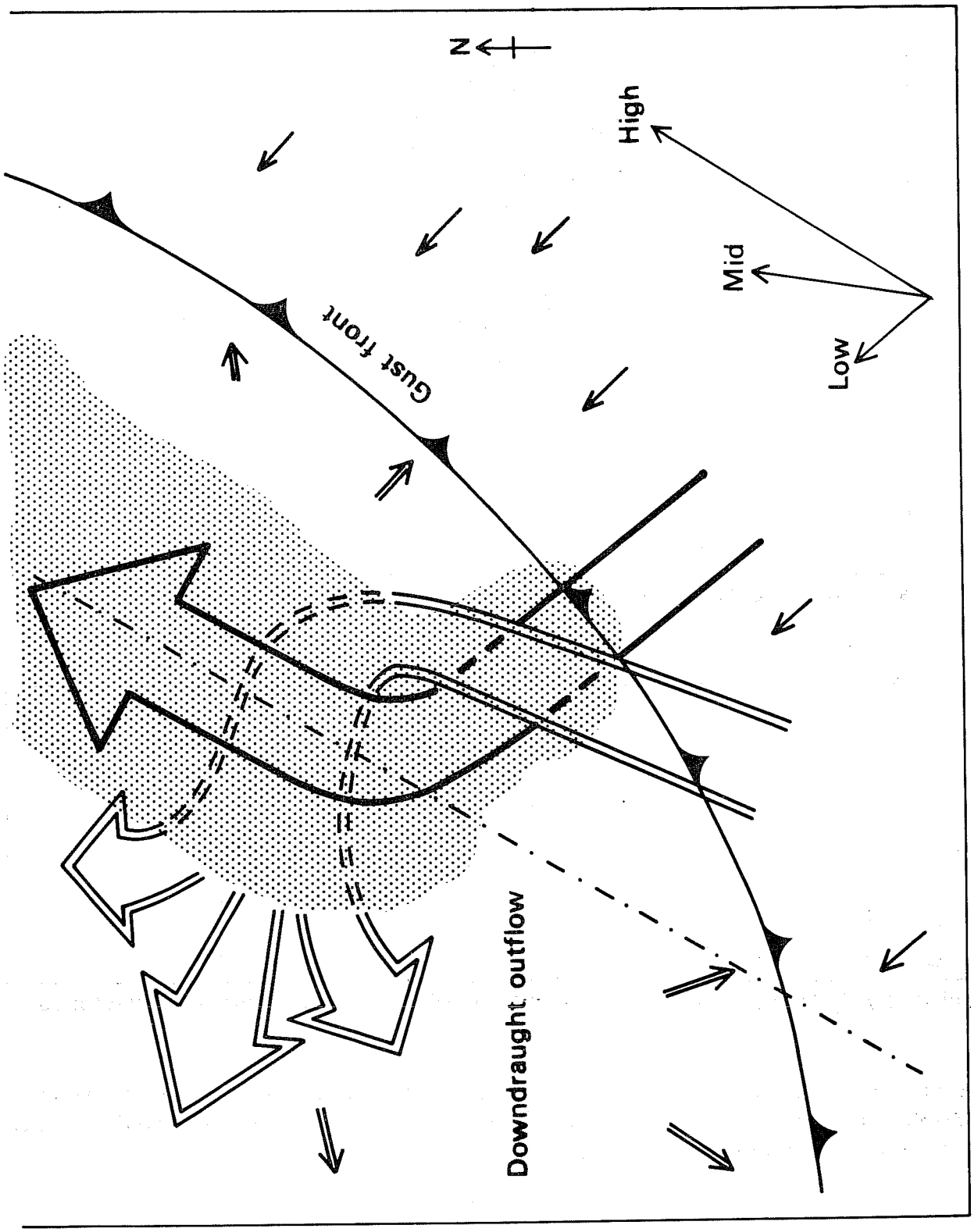

Fig. 4 Schema of 3-D circulation in a simulated storm whose environmental windfield veers with height. This plan view shows the main updraught and downdraught branches together with the ambient windfield.

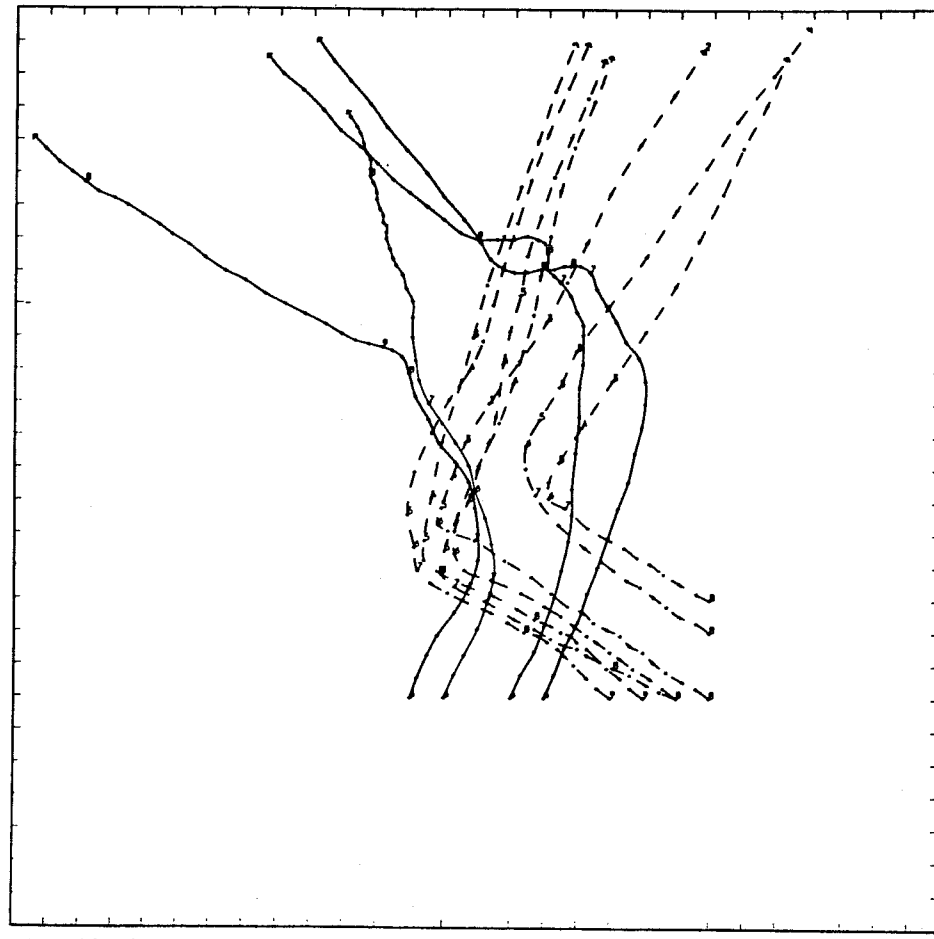

a) Horizontal Multiple Trajectories

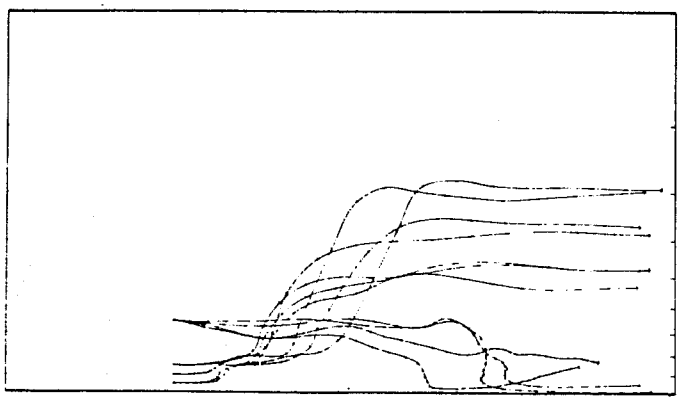

b) Vertical (Y by Z) Multiple Trajectories

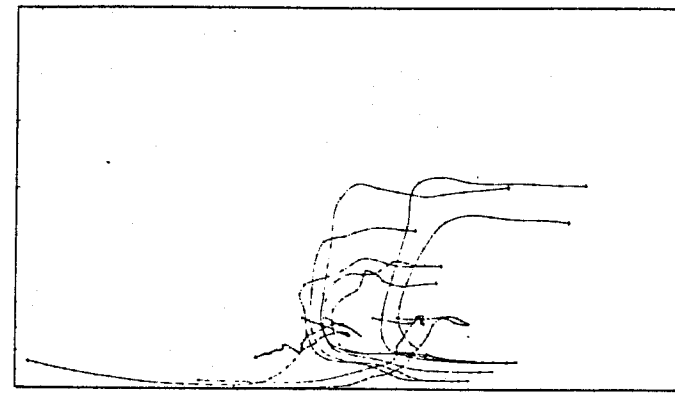

c) Vertical (X by Z) Multiple Trajectories

Fig. 5 Horizontal and two vertical projections of the simulation trajectories on which Fig.4 was based. The two vertical projections show the 'tropical' and 'sheared' components that comprise the 3-D circulation.

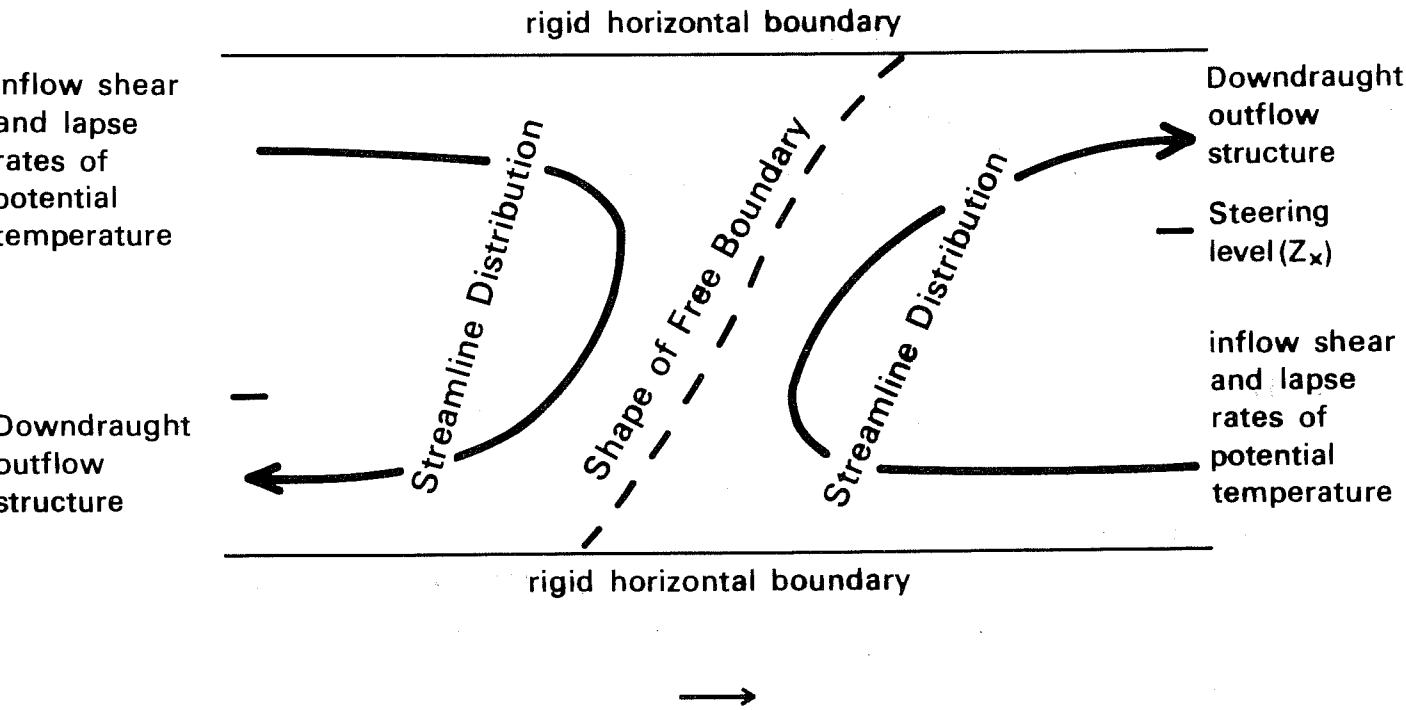

c) Travel speed

Fig. 6 Schema of the specified variables (lower case letters) and the calculated variables (upper case letters) in the mid- latitude model. The diagram is for relative flow.

a) Momentum

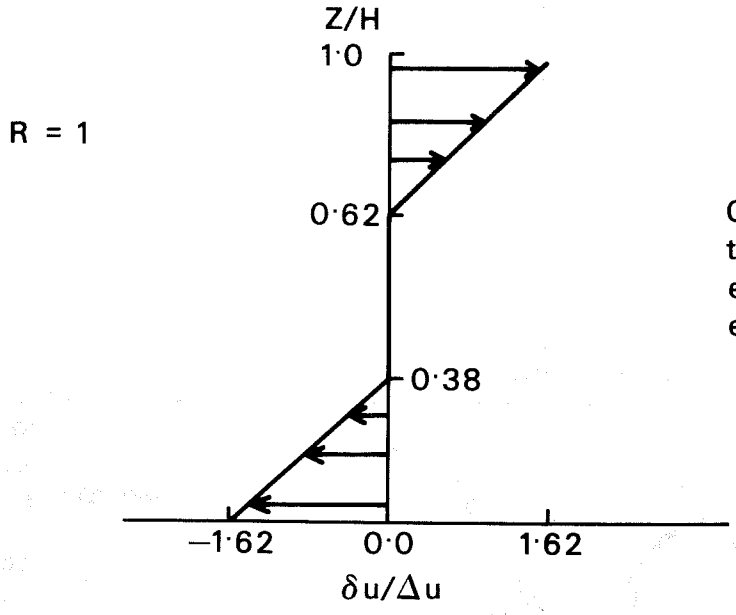

Counter gradient momentum transport; shear and kinetic energy of large-scale flow enhanced

b) Heat

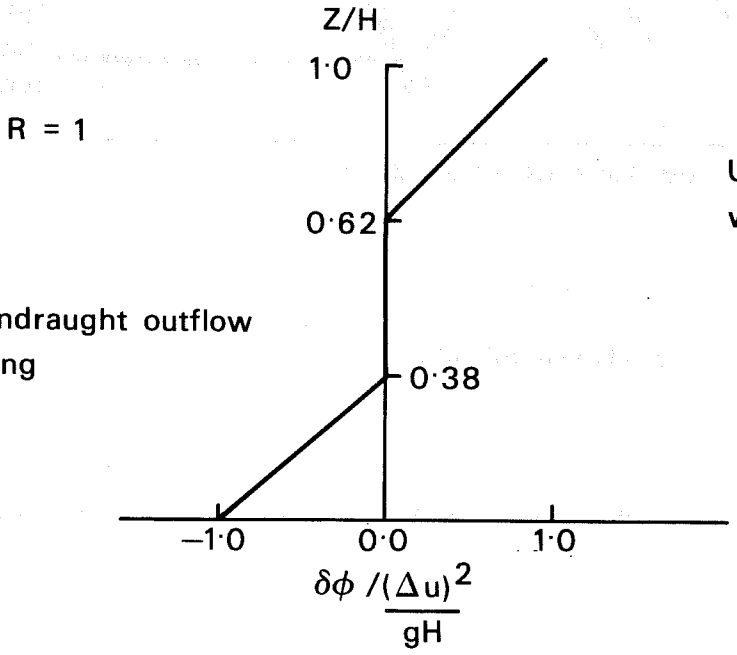

Updraught outflow warming

Downdraught outflow cooling

Fig. 7 Changes effected by the mid-latitude regime in constant undisturbed vertical shear for $R = 1$. (a) Momentum changes (b) Thermodynamic changes. The undisturbed shear is from left to right.

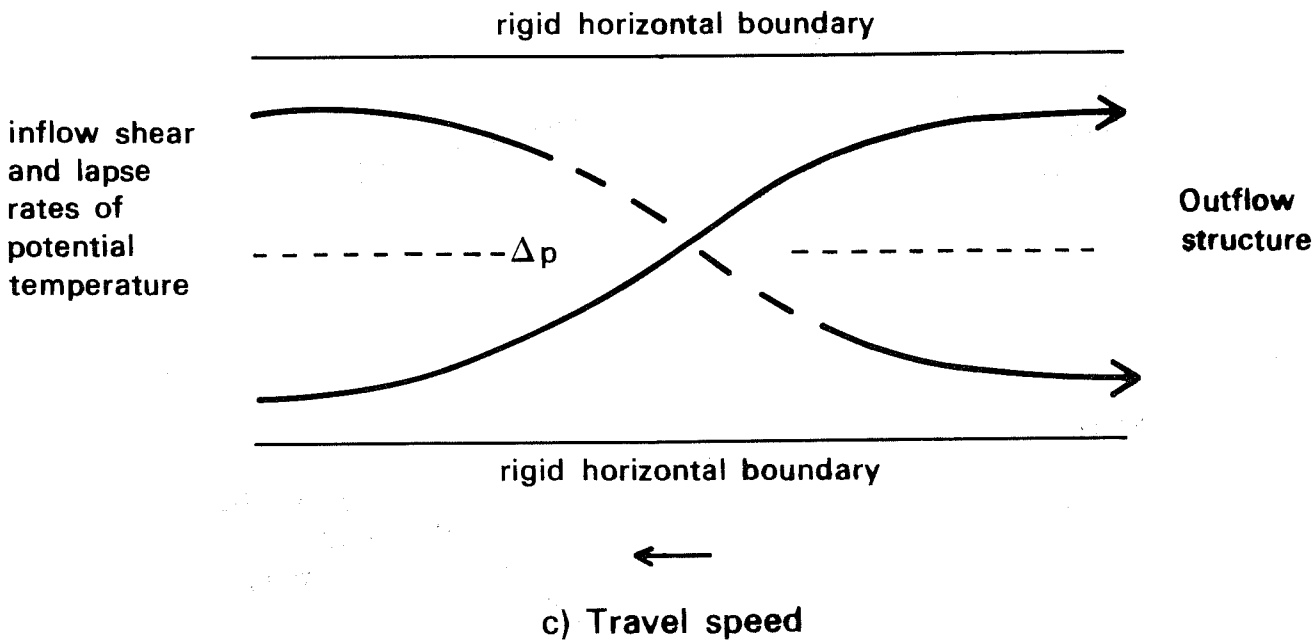

Fig. 8 Schema of the specified variables (lower case letters) and the calculated variables (upper case letters) in the tropical model.

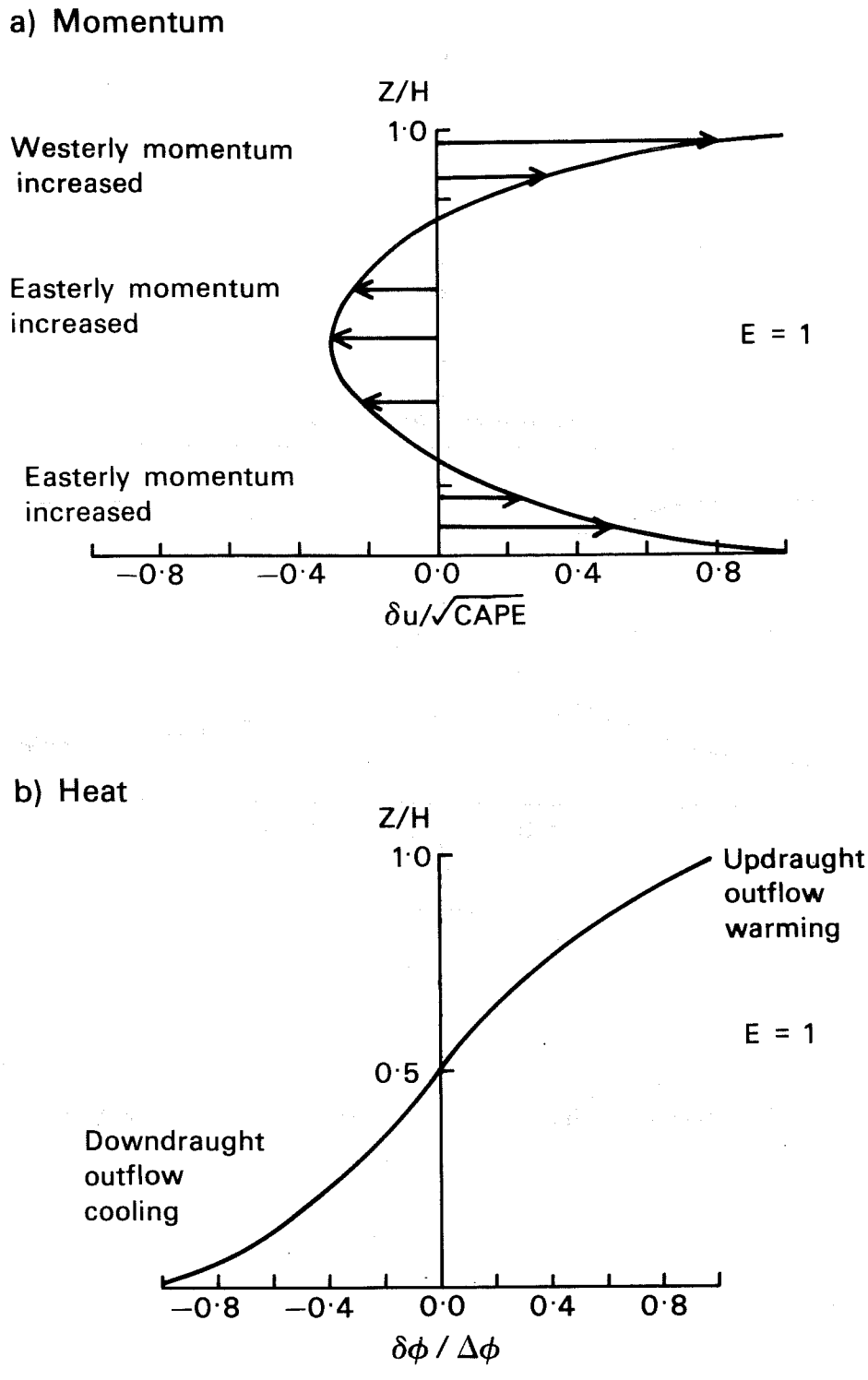

Fig. 9 Changes effected by the tropical regime in zero ambient shear for $E = 1$, where $\Delta\phi = (\gamma - B)H$. (a) Momentum changes (b) Thermodynamic changes.

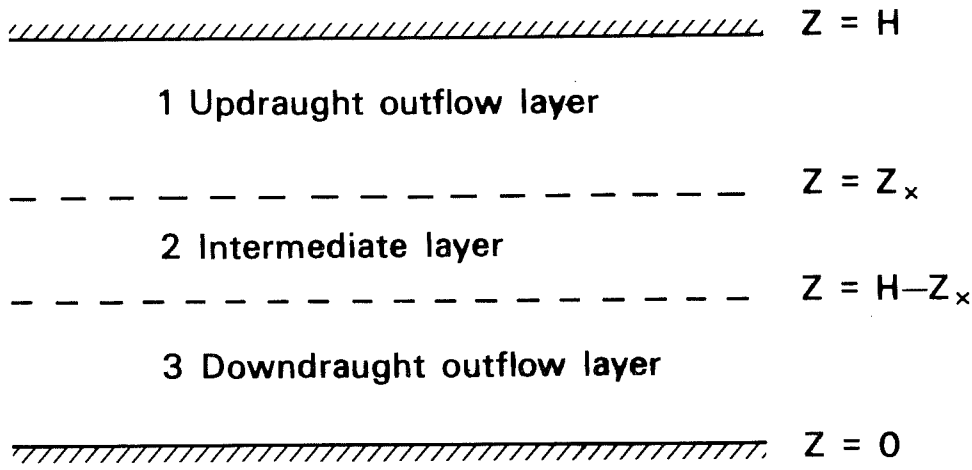

Fig.10 Three layer model applicable to the mid-latitude model transports.